*A Project report on*

# STUDY THE EFFECT OF TEMPERATURE AND CORROSION BEHAVIOR OF RAIL STEEL

*Submitted for partial fulfilment of the requirement of*

**MASTER OF ENGINEERING**

*In*

**METALLURGICAL AND MATERIAL ENGINEERING**

*Submitted by*

**RAJESH DAS (Roll No.:002111302004)**

*Under the guidance of*

**SHILABATI HEMBRAM**
**Assistant Professor**

**METALLURGICAL AND MATERIAL ENGINEERING DEPARTMENT**

**JADAVPUR UNIVERSITY**

**2021-2023**

# Declaration of Originality and Compliance with Academic Ethics

I hereby declare that this thesis, "**STUDY THE EFFECT OF TEMPERATURE AND CORROSION BEHAVIOR OF RAIL STEEL**" contains a literature survey and original research work by the undersigned candidate as a part of my M.E. degree in Metallurgical and Material Engineering during the academic session 2021-2023. All information in this document has been obtained and presented in accordance with academic rules and ethical conduct. I also declare that, as required by these rules and conduct, I have fully cited and referred to all material and results that are not original to this work.

**Name: Rajesh Das**

**Examination Roll Number: M4MET23002**

**Registration No- 136548 of 2016-2017**

**Place-Kolkata**

**Signature**

**Date-**

# CERTIFICATE

This is to be certified by **Mr Rajesh Das (Roll No.: 002111302004, Registration No.: 136548 of 2019-20)**, a final year M. Tech student of the Metallurgical and Material Engineering Department, Jadavpur University, who has completed his project entitled **"**Study the effect of temperature and corrosion behaviour of rail steel". He has submitted his project report for the partial fulfilment of the curriculum for the degree of Master of Engineering in Industrial Metallurgy from Jadavpur University. To the best of my knowledge, the contents of this thesis or any part thereof have not previously been submitted for the award of any degree or diploma.

**----------**

**Prof. Dr. Pravash Chandra Chakraborti**
**Head of the Department**
**Department of Metallurgical and Material Engineering**
**Jadavpur University, Kolkata-700032**

**----------**

**SHILABATI HEMBRAM**
**Assistant Professor**
**Department of Metallurgical and Material Engineering**
**Jadavpur University, Kolkata- 700032**

**----------**

**Prof. Saswati Mazumdar**
**Dean Faculty of Engineering and Technology**
**Jadavpur University, Kolkata-700032**

# Certificate of Approval

The foregoing thesis is hereby approved as a creditable study of an engineering subject and presented in a manner satisfactory to warrant acceptance as a pre-requisite to the degree for which it has been submitted. It is understood that by this approval, the undersigned does not necessarily endorse or approve any statement made, opinion expressed, or conclusion drawn therein, but only the thesis for which it is submitted.

Committee on the final examination for the evaluation of the thesis

---

---

---

Signature of Examiners

# ACKNOWLEDGEMENT

The satisfaction and sense of calmness of the successful completion of any task would be incomplete without mentioning the people who made it possible and whose constant guidance and encouragement crown all efforts with success.

I would like to take this opportunity to express my deep sense of gratitude to my supervisor, Shilabati Hembram, Assistant Professor, Metallurgical and Material Engineering Department, Jadavpur University, for her valuable advice and guidance, constant help and support throughout the period of carrying out the project work, and successful completion of the same in its present form. It was a great experience and privilege for me to work under her in a cordial environment. I would also like to thank all the faculty members for their cooperation and valuable suggestions during the preparation of this report. In the end, last but not least, I want to give special thanks to my parents, family members, and friends for their support and compassion.

# CONTENT

# Abstract

Rail steel is considered one of the most important minerals used in industrial applications. The direct effect on the corrosion behaviour of the steel is heat treatment because of galvanic corrosion, which builds up between its microscopic phases. Four methods of treating carbon steel have been used thermally which are hardening, normalizing, annealing, and tempering. Used salt water as a corrosive medium in the marine environment. The steel contains chemical compounds to show their effect on corrosion. To compare the results with the corrosion rate and weight loss. It was seen that as the carbon content increased, the corrosion durability of the carbon steel decreased. Similar replications of the samples were exposed to annealing heat treatment by heating them and then letting them cool in an isolated furnace. The test results have shown degradation of the sample's corrosion resistance after the heat treatment. Corroded samples exhibited increasing surface area roughness, indicating corrosion defects.


**Keywords: rail steel, annealing, corrosion, the microstructure of rail steel, X-ray diffraction analysis (XRD), microhardness, scanning electron microscope (SEM).**

# 1. Introduction

In this project, it can study how the annealing heat treatment process at specific temperatures will affect the properties of rail steel. Also, shows the corrosion behaviour changes on annealed samples.

Rail steel is a type of steel used in the construction of railway tracks. It is designed to have specific properties that make it suitable for this application. Rail steel is used in a variety of applications, including

- Railway Tracks: Rail steel is primarily used in the construction of railway tracks, including mainline tracks, sidings, and yards. Rail steel provides the structural support required to support train weight and withstand the dynamic forces exerted by moving trains. It is extremely strong, tough, and resistant to wear and deformation.
- Rail steel is used in heavy and high-speed rail: Rail steel is widely used in heavy and high-speed rail systems. Steel with high tensile strength, low deformation under heavy loads, and resistance to fatigue and wear are required for these applications. Rail steel is engineered to meet these specifications while also ensuring the safe and efficient transportation of heavy loads or high-speed trains.
- Rail steel is used in urban transportation systems such as metro rail networks, light rail systems, and tramways. These systems frequently operate in densely populated areas, necessitating rails capable of withstanding frequent starts stops, and turns. Rail steel provides the required durability, wear resistance, and deformation resistance for such demanding environments.
- Rail steel is utilized in industrial environments such as ports, mines, steel mills, and warehouses where specialized rail lines are required for the delivery of large goods. These tracks must be able to survive extreme environments, huge loads, and repeated usage. Rail steel assures the lifespan and dependability of such industrial railway systems.
- Crane Rails: Rail steel is also used in the building of crane rails, which are used at

container ports, shipyards, construction sites, and other areas where heavy lifting and transportation activities take place. Crane rails must be strong, resistant to wear and deformation, and able to endure the impact of huge weights. Rail steel satisfies these standards and offers a sturdy foundation for crane operations. [1]

Rail steel has various unique qualities that make it appropriate for use in railway rails. Rail steel's primary features include:

- High Strength: Rail steel is designed to be strong enough to carry the weight of trains while also resisting the stresses caused by moving loads. It can resist high loads without substantial deformation or failure.
- Toughness: Rail steel has high toughness, which allows it to absorb and release energy from impact loads such as wheel-rail contact. This quality helps to inhibit fracture propagation and preserve the rail's long-term integrity.
- Rail steel is designed to have a high wear resistance owing to repeated contact between the train's wheels and the rail surface. It can endure the abrasive forces caused by rolling contact while minimizing wear and material loss over time.
- Fatigue Resistance: Over its service life, rail steel is subjected to millions of load cycles, which can lead to fatigue failure if not adequately engineered. Rail steel is specially designed to be fatigue-resistant, allowing it to bear cyclic loads without cracking or failing.
- Ductility: Rail steel has some ductility, which permits it to go through plastic deformation without shattering under large loads. This feature is critical for preserving the structural integrity of the rail and preventing catastrophic breakdowns.

# 2 Definition of the problem:

This project teaches how the annealing heat treatment process at different temperatures affects the physical properties of rail steel. Also, shows the corrosion changes on annealed samples.

In previous research work, three methods of thermally treating carbon steel were examined: annealing, normalizing, and hardening. 30 days, 45 days, and 60 days of using salt water as a corrosive medium. Chemical elements in the steel demonstrate how corrosion is affected by them. Weight loss was used to assess the corrosion rate, compare results, and make comparisons. The results obtained demonstrate that the corrosion resistance of hardened steel is the lowest, that of annealed steel is the greatest, and that of normalized steel is intermediate. The corrosion rates of hardening samples were 0.061 (30 days), 0.063 (45 days), and 0.0962 (60 days). The corrosion rates of normalizing samples were 0.0652 (30 days), 0.065 (45 days), and 0.0823 (60 days). The corrosion rates of annealing samples were 0.056 (30 days), 0.062 (45 days), and 0.08 (60 days) [2].

In another paper, it has been observed that heat treatment processes and corrosion rates are studied for rail steel samples. In a paper, samples with different carbon contents (0.08, 0.15, 0.2, 0.3, and 0.4%) were considered to establish corrosion characteristics. The corrosion effect was investigated by exploring the results of the corrosion effect using the Mlab200 potentiostat Tafel on the Tafel principles of polarization. It was seen that as the carbon content increased, the corrosion durability of the carbon steel decreased. Similar replications of the samples were exposed to annealing heat treatment by heating them to 850 °C for 17 minutes and then letting them cool in an isolated furnace [4].

After reviewing the previous research work, the 0.6% C Rail steel was used as an experiment sample, and annealing heat treatment was chosen because it has a lower corrosion rate than other heat treatment processes. That's why furnace cool annealed heat treatment is chosen at four different temperatures, like 1005 °C, 910 °C, 810 °C, and 705 °C, and we're trying to find out how to decrease the corrosion rate of rail steel.

The reason behind the aim of this project is that railway tracks are placed in many places where highly corrosive media are present. That's why if rail steel has a lower corrosion rate, it will help the railway department reduce accidents or damage caused by corrosion.

# 3 OBJECTIVE

The research aims to study the effects of various heat treatment temperatures, like 1005 °C, 910 °C, 810 °C, and 705 °C. Also, the objective is to study the corrosion behaviour of rail steel (high carbon steel) base material and heat-treated substrate in a 3.5 wt% NaCl solution.

# 4 Plan of Work:

1. An Optical Microscope was used for the given base sample and the four heat-treated samples for observation of the microstructure.
2. X-ray diffraction analysis (XRD) of the given base sample and the four heat-treated samples was used to identify materials based on their diffraction pattern and crystallographic phases.
3. Annealing is used for the given rail steel sample to eliminate internal stresses and improve the hardness.
4. Energy dispersive spectroscopy enables the chemical characterization/elemental analysis of materials for the given base sample and the four heat-treated samples
5. Vickers Hardness Testing is used for the given base sample and the four heat-treated samples to measure the hardness of a material, calculated from the size of an impression produced under load by a pyramid-shaped diamond indenter.
6. Perform corrosion test analysis to study the corrosion behaviour of the base material and heat-treated samples of rail steel.
7. A scanning electron microscope is used to study the metallographic phases and the corrosion effects of the base material and heat-treated samples of rail steel.
8. Perform corrosion test analysis with sulfuric acid at three different pH levels (1.5, 2.7, and 3.9) to study the corrosion behaviour of the base material and heat-treated samples of rail steel.

# 6 Literature review:

## *6.1 History:*

The development of railroads, which revolutionized transportation and played a vital role in the Industrial Revolution, is entwined with the history of rail steel. Rail steel is a kind of steel used in the building of railway tracks to provide a long-lasting and dependable basis for train operations.

Rail steel may date back to the early nineteenth century. The original railways were made of wooden rails or stone blocks, which were easily worn and damaged. Stronger and more durable materials were required as the need for quicker and more efficient transportation increased.

The first cast iron rails were added in 1820, which improved on the earlier wooden and stone constructions. Cast iron rails were more durable and resistant to wear, but they remained fragile and prone to breaking under severe loads.

The adoption of wrought iron rails in the 1830s was the next great innovation. Iron ore was smelted in a furnace and then hammered to eliminate impurities and form it into rails to make wrought iron. Wrought iron rails were stronger and more robust than cast iron rails, making them more suitable for the growing needs of railway traffic. They could resist heavier weights and last longer.

Wrought iron rails, on the other hand, have restrictions. They were heavy and expensive to make, making railway construction expensive. Steelmaking methods advanced significantly in the mid-nineteenth century, resulting in the introduction of steel as a superior material for rail building.

The Bessemer method, developed by Sir Henry Bessemer in the 1850s, enabled low-cost mass manufacturing of steel. To eliminate impurities and manufacture steel with suitable qualities, the air was blown through molten pig iron. The Bessemer process transformed steel manufacturing and made it more widely available for use in a variety of applications, including railway tracks.

The advent of steel rails benefited the railway business in a variety of ways. Steel rails were more robust, stronger, and more resistant to wear and deformation. These allow for faster train speeds, larger loads, and fewer maintenance requirements. Steel rails also allowed trains to expand into more difficult terrains, such as hilly regions.

Advances in steelmaking technology and metallurgical understanding have enhanced the quality of rail steel throughout the years. Contemporary rail steel is designed particularly to withstand the demands of high-speed trains, large goods movement, and a variety of environmental conditions.

Finally, the growth of railway infrastructure is reflected in the history of rail steel. Rail steel has evolved from timber and stone rails through cast iron and wrought iron, and eventually to steel.

### *6.2 Properties of rail steel:*

Rail steel has various unique qualities that make it appropriate for use in railway rails. Rail steel's primary features include :

1. **High Strength:** Rail steel is designed to be strong enough to carry the weight of trains while also resisting the stresses caused by moving loads. It can resist high loads without substantial deformation or failure.
2. **Toughness:** Rail steel has high toughness, which allows it to absorb and release energy from impact loads such as wheel-rail contact. This quality helps to inhibit fracture propagation and preserve the rail's long-term integrity.
3. **Wear Resistance:** Rail steel is designed to have a high wear resistance owing to repeated contact between the train's wheels and the rail surface. It can endure the abrasive forces caused by rolling contact while minimizing wear and material loss over time.
4. **Fatigue Resistance:** Over its service life, rail steel is subjected to millions of load cycles, which can lead to fatigue failure if not adequately engineered. Rail steel is specially designed to be fatigue-resistant, allowing it to bear cyclic loads without cracking or failing.
5. **Ductility:** Rail steel has some ductility, which permits it to go through plastic deformation without shattering under large loads. This feature is critical for preserving the structural integrity of the rail and preventing catastrophic breakdowns.

### *6.3 Application of rail steel:*

Rail steel is used in a variety of applications, including:

- ➢ Railway Tracks: Rail steel is primarily used in the construction of railway tracks, including mainline tracks, sidings, and yards. Rail steel provides the structural support required to support train weight and withstand the dynamic forces exerted by moving trains. It is extremely strong, tough, and resistant to wear and deformation.
- ➢ Rail Steel Is Used in Heavy and High-Speed Rail: Rail steel is widely used in heavy and high-speed rail systems. Steel with high tensile strength, low deformation under heavy loads, and resistance to fatigue and wear are required for these applications. Rail steel is engineered to meet these specifications while also ensuring the safe and efficient transportation of heavy loads or high-speed trains.
- ➢ Rail steel is used in urban transportation systems such as metro rail networks, light rail systems, and tramways. These systems frequently operate in densely populated areas, necessitating rails capable of withstanding frequent starts stops, and turns. Rail steel provides the required durability, wear resistance, and deformation resistance for such demanding environments.
- ➢ Rail steel is utilized in industrial environments such as ports, mines, steel mills, and warehouses where specialized rail lines are required for the delivery of large goods. These tracks must be able to survive extreme environments, huge loads, and repeated usage. Rail steel assures the lifespan and dependability of such industrial railway systems.
- ➢ Crane Rails: Rail steel is also used in the building of crane rails, which are used at container ports, shipyards, construction sites, and other areas where heavy lifting and transportation activities take place. Crane rails must be strong, resistant to wear and deformation, and able to endure the impact of huge weights. Rail steel satisfies these standards and offers a sturdy foundation for crane operations.

### *6.4 Previous research work based on rail steel corrosion behaviour*

There is a difference in the corrosion rates for different heat treatments. At 30 days, the lowest corrosion rate was obtained for carbon steel heat treated by annealing, followed by carbon steel heat treated by hardening, and finally, steel treated by normalizing. After 45 days, the corrosion rates of the heat-treated steel by annealing increased very slightly, while the corrosion rates remained constant for both the heat-treated steel by hardening and normalizing. At 60 days, the corrosion rates differed for all types of carbon steel, as the results showed that the hardening-treated steel obtained the highest corrosion rate, followed by the carbon steel treated by normalizing, and the lowest corrosion rate for the carbon steel treated by annealing.

As for carbon steel treated with the formula, the increase in the corrosion rate is due to its effect on the microstructure and the number of cells, as the microscopic cells are small in size and numerous in number when compared to fermentation treatment. Whenever the number of microscopic cells is large and they are small in size, the rate of erosion will be high because the increase in the number of cells with their small sizes leads to an increase in the areas of potential difference between the cells and the boundary and thus increases the corrosion rate.

Annealing-treated steel is slowly cooled down by keeping the models in the oven, and this allows more time for cell growth than cooling by other methods. Corrosion medium is one of the important factors that affect the speed of corrosion rates, especially salt water because the chloride ions present in salt increase the electrical conductivity, which leads to acceleration of the corrosion process.

Heat treatments have an effect on corrosion rates through their effect on the microstructure and the number of galvanic corrosion cells between microscopic phases or between microscopic cells and their boundaries. Whenever the number of microscopic cells is large or small, the corrosion rate is high because the increase in the number of cells leads to an increase in the areas of potential difference between the cells and their borders, and thus an increase in the corrosion rates.

The highest corrosion rates were in hardening steel due to the stresses it was exposed to during water quenching, and the lowest corrosion rates were in annealing-treated steel

due to the microstructure of heat-treated steel. Corrosion medium is one of the important factors that affect the speed of corrosion rates, especially salt water because the chloride ions present in salt increase the electrical conductivity, which leads to an acceleration of the corrosion process. **[2]**

The corrosion rate, weight loss and electrode potential for the normalized low-carbon, medium-carbon and high-carbon steel samples immersed in a 3.5M NaCl solution are shown. At an earlier stage of immersion, the corrosion rate of the samples as shown increased sharply and immediately decreased before it began to increase again, except for the medium carbon steel, which continued to increase until the 10th day. The high carbon steel was observed to increase in its corrosion rate and started to decrease uniformly on the 15th day until the end of the immersion test, in contrast to the low and medium carbon steel samples, which decreased on the 10th day and were seen to increase on the 27th day until the end of the immersion test.

The high carbon steel sample shows the least weight loss in comparison with the medium carbon steel sample, which showed the least weight loss at the earlier stage of immersion and increased uniformly on the 13th day until the end of the immersion test. The earlier stage of immersion of the three steel samples showed an increase in electrode potential and decreased on the third day until the 34th day when all three steel samples also increased in their electrode potential. Between the 3rd and 52nd days, the high-carbon steel electrode potential is observed to increase before decreasing sharply until the end of the immersion test.

The corrosion rate, weight loss and electrode potential plots for the annealed low-carbon, medium-carbon and high-carbon steel samples, immersed in a 3.5M NaCl solution. The earlier stage of immersion shows an increase in the corrosion rate of the three steel samples. Between the 3rd and 24th days, there was an increase in the corrosion rate of the high carbon steel, although it was lowest compared to that of the low and medium carbon steels with higher corrosion rates, which decreased for the medium carbon steel until the 34th day. However the low-carbon steel experienced a rise and fall in its corrosion rate between the 3rd and 10th days, and it decreased thereafter until the end of the immersion test. The high-carbon steel shows the lowest corrosion rate. **[3]**

Annealing heat treatment of different carbon contents of carbon steel with opposing corrosion characteristics has been considered. Carbon steel samples with different carbon contents were tested by exposure to corrosive media. The results showed that as the carbon percentages increased, less corrosion durability was exhibited by the steel due to the excessive amount of perlite corrosive cells. Moreover, exposing the carbon steel samples to annealing heat treatment resulted in more corrosion than the unheated samples. The non-crystal deposited grains were noticed to cause surface defects, leading to more corrosive action and surface roughness.

A feasible idea will be to consider high-carbon steel with normalizing heat treatment, considering corrosion tests. Other metals, such as aluminium, copper, etc., can be tested before and after the annealing process for corrosion effects. **[4]**

A detailed analysis of the material properties found in this project could help support existing findings. For example, the correlation found between hardness and ultimate tensile strength may help to support claims that hardness tests can be used as a means of also finding the

ultimate tensile strength magnitude, which is a useful finding for saving money when testing rail

steels. The material analysis conducted within this project also shows that yield strength is vastly different between the head and foot of a rail, as evidenced in. The maximum difference is as high as 24% This could be investigated in another study to see if this has any effect on the life cycle of a rail and the reasons behind this phenomenon. It is speculated in this study that the heat treatment of samples was the reason for such discrepancies in results. The data showed that HP335, a non-heat-treated specimen, had no difference in yield strength at the head and foot, while the other specimens exhibited large differences. The cooling rate of heat-treated samples is said to have a large impact on the yield strength of a material. Comparing material properties to wear within this report has yielded evidence for a potential method of predicting wear rate, that includes material properties that have not been considered in previous railway wear models. The understanding that a ratio of Young's modulus squared and percentage elongation to

hardness cubed ((E2*Pe)/H3) could have a potentially large impact on the wear resistive properties of rail steel is of high value to the rail industry, with regards to maintenance costing and scheduling. The implications of this project could lead to further testing to prove the model's repeatability and accuracy for use in the industry and could help to update current damage prediction models. Comparing material properties to rolling contact fatigue (RCF) in this project, led to new ideas for characterizing Mark Burstow's whole life rail model (WLRM). Findings in this report showed that a potentially stronger correlation existed between ultimate tensile strength (UTS) and RCF resistance (R2 =1.0) than between hardness and RCF resistance (R2 =0.975). This led to the idea that Mark Burstow's WLRM material characterization equations may be more accurate when UTS is included instead of hardness, as can be seen in equations 14 and 15 compared to equations 10 and 11. The UTS data was taken by averaging the UTS of samples from the head and foot of the rail. The material properties found in the tensile test conducted for this study and used in this analysis, may not be an exact match to the material properties of the samples used by Burstow to gather his data. It would be interesting to see further research on this, as other material properties such as fracture strain, yield strength, and a ratio of H3/(E2*Pe) also showed a better correlation to the RCF resistance data than hardness. This may show that ductility and toughness properties must be considered to predict RCF crack initiation and wear properties, not just hardness. Furthermore, the ability of a material to resist fracture may also be an important parameter in determining the RCF resistance of a material. The new wear model discussed in this project also supports this statement. **[5]**

This study primarily focused on the material responses of worn-out rail steel in terms of its hardness

profile and microstructure variations. The study clearly depicts the consequence of basic pearlitic steel on rails to generate hardness distribution, indicating a softer core confined to harder outer surfaces. The microstructure observation reveals the influence of rolling contact fatigue induced by thermomechanical loading, which develops wear by forming more and more of a softer ferrite distribution with the harder cementite layer moving closer to the outer surface. The consequence of such a cementite portion is that it helps

crack initiation and propagation by branching out in the cementite region only. The contribution of RCF, thus obtained, can be utilized to design a better material and to formulate a more appropriate safety strategy based on the discussed results in the study. **[6]**

Rail steel production involves the proper combination of alloying elements and heat treatment, resulting in a wide range of grades with varying hardness and wear resistance. The rail grade chosen by a railway is based on traffic and track conditions, and excellent service life can be achieved, especially if modern rail head lubrication and grinding practices are used. This research is concerned with changing the standard heat treatment, which is based on traditional pearlitic steel, in order to save energy during production. As a result, the investigated R350HT steel was subjected to isothermal heat treatment, which included hardening to achieve a bainitic microstructure. The steel was then annealed, after which it was further cooled in a furnace before final cooling. The steel was then annealed. Following this, a further cooling process with a furnace was followed by a final cooling process in the air. The Zeiss light metallographic microscope and the scanning electron microscope were used to examine the steel's microstructure. Additionally, a tribometer was used to conduct friction wear tests and Vickers microhardness examinations on sample cross-sections. Additionally, a Charpy impact toughness test was run at room temperature to assess the mechanical qualities that were attained. Based on the analysis of the light microscope structure investigations, it was discovered that the R350B steel's microstructure was made up of relatively large irregular grains. The mechanical properties investigations' results show only a modest increase in hardness and wear compared to the traditional 350 HT steel, the 350B steel has higher resistance. However, the current ferritic structure reveals some advantages related primarily to lower energy consumption during heat treatment, with hardness and wear resistance values nearly on par with those of the 350 HT steel. The obtained results have not confirmed the existence of the bainitic structure in the 350B steel. **[7]**

The goal of this paper is to conduct an experimental study on the fatigue fracture performance of rail steel used in Iran's railways. Fatigue, fracture toughness, and fatigue

crack growth tests were performed for this purpose, and the results were validated by fractography studies on fractured specimens because of fatigue failure,

Because it occurs in micro dimensions, it can be used for fracture surface analysis and the study of nonmetallic inclusion distribution. The experimental results serve as a good foundation for evaluating the numerical results, and they have been used to assess the structural continuity of rail steel in railway networks.

In this study, the mechanical properties and fatigue fracture performance of rail steel in Iran's railway are presented on an experimental basis, with the results accurately calculating the fatigue life of rail components such as rail in the shortest time, lowest cost, and largest volume of calculations. Fractography studies were then performed on fractured specimens. The goal of this research is to conduct a 505 study on the fatigue fracture performance of rail steel used in rail networks. The following are the most important findings of this study:

1. Rail steel's high strength and ductility, as well as its high strain hardening capacity.

510 2. Rail steel demonstrated high fatigue strength based on a flat S-N curve with a high fatigue limit slightly higher than the material's yield point. Furthermore, the fatigue failure mode of this rail steel is cleavage, which generally results in the material's brittle behaviour.

515 3. In terms of pop-in behaviour during crack growth and cleavage fracture surface characteristics, the fracture toughness of rail steel is lower than that of pearlitic rail steel, similar to that used for rails.

4. Based on the large amounts of crack growth rate parameter 520 (n) and brittle material behaviour obtained from the experimental results, it can be concluded that rail steel resistance to fatigue crack growth is low. Furthermore, low KIcof steel results in poor damage tolerance behaviour.

5. The critical crack length in the rail is calculated to be 37 mm. It is obvious that the critical crack length will change at different temperatures and operating conditions, such as residual stresses and axial loads. **[8]**

Pearlitic microstructures continue to dominate railway tracks, despite competition from bainitic and martensitic steels. Techniques developed in recent years have refined the

interlamellar spacing, resulting in harder, more wear-resistant pearlitic steels. The purpose of this research is to explain the mechanisms underlying wear performance by observing how the microstructure adapts to wear loading.

Four pearlitic rail steels with similar chemical compositions but varying interlamellar spacings were investigated. Wear tests were carried out under both pure sliding and rolling-sliding conditions, with the latter intended to simulate track conditions. Optical metallography and scanning electron microscopy were used to examine the worn surfaces and plastically deformed subsurface regions.

The plastic deformation caused significant fracturing and realignment of the hard cementite lamellae. When approaching the worn surface, the softer ferrite matrix was severely deformed, allowing for a reduction in interlamellar spacing. These surface realignments resulted in an increased area fraction of hard cementite lamellae on planes parallel to the surface. Thinner cementite lamellae with small interlamellar spacings bent more easily before fracturing. Shear ductility is thought to play an important role in the amount of time a given volume of material remains at the surface before becoming a loose particle. **[9]**

For the purpose of resolving rolling contact fatigue (RCF)—contact mechanics issues—the significance of material properties is demonstrated. The role of the material in the system is crucial in addition to factors like friction, loading, and geometry. In the field of contact mechanics, there are still unanswered questions regarding the determination and modelling of these material properties under the typical load conditions of a wheel-rail contact. A closer look at these material properties could contribute to a global solution.

In the scientific field of contact mechanics, material properties developing under the unique circumstances of wheel-rail contact are regarded as almost "unknown territory." A closer examination of material properties may reveal the crucial piece that completes the extensive and complex work done so far for the wheel-rail system in all other contact mechanics disciplines. One prerequisite for reaching this target is having a closer look at the validation of the models. The three system partners—universities, businesses, and

infrastructure owners—must work closely together on this. When simulation work and model development at universities also consider data from real tracks and materials, the goal of system improvement will be more effectively achieved. Models and theories must account for the actual behaviour of various rail steel grades in various operational circumstances. Operators of both the industry and the infrastructure can provide this information. **[10]**

Pearlite spheroidization is a metallurgical process in steels in which cementite lamellae break down into spheroids, causing the samples' Vickers hardness to decline. In this work, alternative approaches for detecting cementite particle length and breadth via scanning electron microscopy are examined in micrographs. A ribbon-like approach for quantifying particles is presented based on a test image length and width, as well as distinguishing lamellae from spheroids. There are many heat-treated samples produced and characterised. The analytical results are utilised to justify the evolution of the microstructure of the samples. It is demonstrated that, when compared to the standard DeHoff form factor, fresh insight into the spheroidization process is discovered by analysing the distributions of lamellar length and breadth.**[11]**

The silicon level ranged from 0.25 wt.% to 2.00 wt.%, but the concentrations of the remaining alloying elements in the steels were almost identical. It is worth noting that 0.25Si steel is equal to commercial 100Cr6 bearing steel. All of the steels were created via vacuum ingot casting with high-purity alloying metals, resulting in ingot diameters of 120 120 500 mm3. Following casting, the ingots were homogenised at 1230 °C for 5 hours before being hot rolled into wires 10 mm in diameter. The steel's as-rolled microstructures from which the totally pearlitic structure was formed. The interlamellar spacing in the steels varies slightly: 0.32 m for 0.25 Si, 0.30 m for 1.00 Si and 1.50 Si, and 0.29 m for 2.00 Si steel, respectively. In reality, this is critical because it is required to rule out any factors other than silicon concentration that might alter cementite's spheroidizing behaviour, which is significantly dependent on interlamellar spacing. The annealing temperature was adjusted from 790 °C to 850 °C during the spheroidization process. After 6 hours of heating, the steels were gently cooled to 735 °C at a rate of 45

°C/h and subsequently to 670 °C at a rate of 10 °C/h. The specimens for microstructural investigations were etched and inspected with a JEOL JSM-7000F field-emission scanning microscope. The electron microscope. All specimens' Vickers hardness was determined using the Mitutoyo automated microhardness tester HV114 testing system with a 1-kilogramme load. The hardness displayed is an average of at least five readings. ThermoCalc was used to do the thermodynamic calculations. TCCR version software and the TCFE2 database, as well as a result, the pseudo-binary phase diagram and variants of Carbon activity, were measured with various silicon concentrations**[12]**.

In a simulated industrial atmosphere, the corrosion behaviours of Q345B carbon steel and S500AW railway steel for railroads were assessed, and the corrosion mechanism of S500AW railway steel was investigated. Periodic immersion corrosion studies were performed on two kinds of steel for 24 hours, 120 hours, 240 hours, and 360 hours. The weight loss technique was used to calculate corrosion weight loss and corrosion rate. Electrochemical tests were used to examine the corrosion potentials and corrosion current densities of two kinds of steel throughout four cycles. The corrosion behaviour of Q345B and S500AW was evaluated using macromorphology, micromorphology, and corrosion product composition. In periodic immersion corrosion trials, the corrosion rate of S500AW was lower than that of Q345B. The fraction of -FeOOH in the rust layer rose as the experiment duration was extended. The corrosion resistance of S500AW was higher than that of Q345B in the simulated industrial environment. During the 360-hour immersion trials, the value of Q345B grew at first and then looked to remain stable, but the value of S500AW increased**[13]**.

The corrosion of pearlitic rail steel in various settings has generated the following results:
1. In a maritime environment, both yield and tensile strength drop as the corrosion rate increases.
2. In an acidic environment, yield is related to corrosion rate, whereas tensile strength is proportional to corrosion rate.
The aforementioned corrosion and mechanical tests on pearlitic rail steel in various environmental situations show that, because the mechanical characteristics of the

aforesaid steel decline dramatically owing to environmental corrosion, frequent in-situ metallographic testing is required. Failure study of the rails suggests that thorough examination is required to avoid early failure of the rails. Rail tracks constructed of pearlitic steel may be replaced in very aggressive corrosion zones such as seacoast locations and large subterranean tunnels with bainitic rail steel, which is believed to have greater mechanical qualities than pearlitic rail steel **[14]**.

The literature on rail track corrosion has been studied, covering corrosion forms, corrosion prevention, and detecting systems. On a vast rail surface, general corrosion would not be a concern, but crevice corrosion between rail and liner poses a possibility of rail foot thinning. Reciprocating micromotion between rail foot and liner would mechanically aid in the onset and continuation of crevice corrosion, despite the fact that this has only been briefly proposed by a few studies with insufficient follow-up. We believe that crevice corrosion should be studied under both static and micro-dynamic situations; otherwise, this corrosion problem will continue to be a potential danger to rail track service life and safety. Furthermore, DC deviate 10 W. Rail track corrosion and protection, Xu et al. Current corrosion is also a key factor in rail track degradation, particularly for the rail base and rebar in the concrete slab. Coating (painting) can successfully boost rail track corrosion resistance, but it currently has a flaw in the form of poor mechanical qualities, particularly for the intensive contact between the rail surface and wheels. Surface modification technologies such as thermal spraying and laser cladding should be able to overcome the flaw while also maintaining a good corrosion-resistant layer, but the exact cost is unknown. Another efficient method is to create new rail steel, however, the unavoidable loss of mechanical qualities while boosting corrosion resistance can occasionally constitute an impediment to future practical usage. Instead of focusing just on corrosion, we believe that the synergistic impact of corrosion resistance and mechanical property should be the study focus. Corrosion detection technology development is as important as corrosion research on rail tracks, particularly in-situ nondestructive and contactless technologies. Ultrasonic detection and infrared inspection have been employed in practice and several sophisticated fault detection technologies that have been used in other circumstances show promise for rail track inspection**[15]**.

# 7 Experiment methods

## *7.1 Sample preparation:*

When preparing samples for microscopy, it is important to produce something that is representative of the whole specimen. It is not always possible to achieve this with a single sample. Indeed, it is always good practice to mount samples from a material under study in more than one orientation. The variation in material properties will affect how the preparation should be handled; for example, very soft or ductile materials may be difficult to polish mechanically.

Cutting a specimen

It is important to be alert to the fact that the preparation of a specimen may change the microstructure of the material, for example, through heating, chemical attack, or mechanical damage. The amount of damage depends on the method by which the specimen is cut and the material itself. Cutting with abrasives may cause a large amount of damage, whereas the use of a low diamond saw can cause fewer problems.

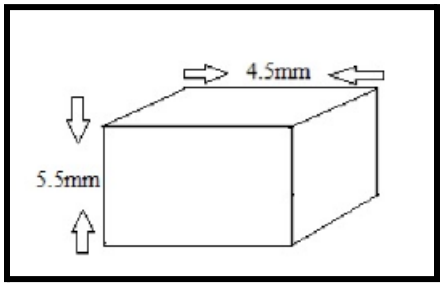


Fig. 1: The size of cutting samples of rail steel

## *7.2 Heat treatment:*

It is heating the metal to a certain temperature, holding it at that temperature for a period of time, and then cooling it at a specified rate. Heat treatment processes are carried out to change the properties of the metal, including: increasing hardness, ductility, and toughness, increasing the metal's ability to form and work processes; removing internal stresses resulting from working processes; and removing the effects of cold forming

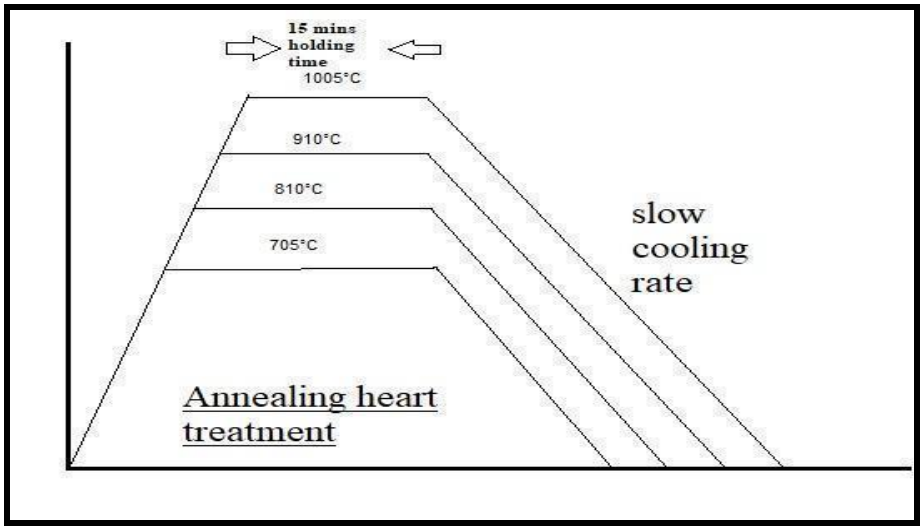


Fig. 2: Heat treatment graph of the annealing process with selective temperatures

processes. Heat treatment processes that were used in this research include: annealing (Fig. 2).

- Preheating the furnace to the desired temperatures of 1005, 910, 810, and 705 degrees Celsius
- Inserting the rail steel samples into the furnace with the proper handling equipment.
- Ensuring an even distribution of temperature throughout the boiler.
- Holding the samples for a set period of time—15 minutes—at the aforementioned target temperatures.
- Keeping an eye on and managing the temperature to reduce temperature changes.
- Reducing sample oxidation and oxygen exposure to a minimum.

## *7.3 Microstructure observation using an optical microscope:*

A metallurgical microscope with accessories for image analysis was used for the optical microscopic investigation of the rail steel samples. The specimens for the test were metallographically polished and etched before microscopic examination was performed. Magnification 100x, 200x, 500x and 1000x are used in the optical microscope for all samples

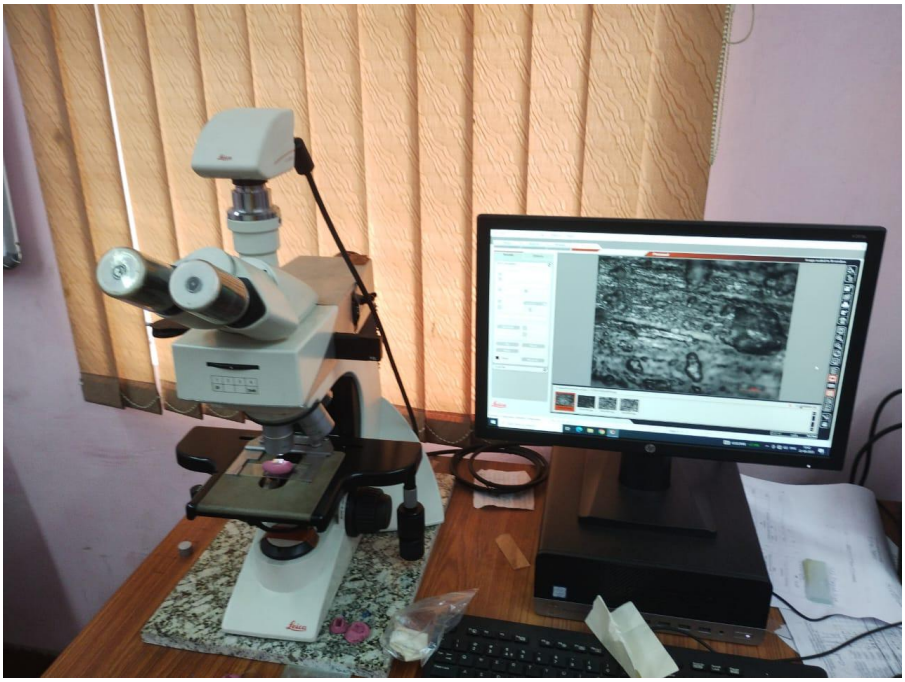

Fig. 3: Leica DM2000 Ergonomic system microscope

### *7.4 X-ray diffraction analysis*

Size Selection of Specimens:

Choose representative samples of the item you want to analyze with X-ray diffraction. Make sure the samples are 5 mm in height and 4.5 mm in width on the XRD instrument's sample holder or stage.

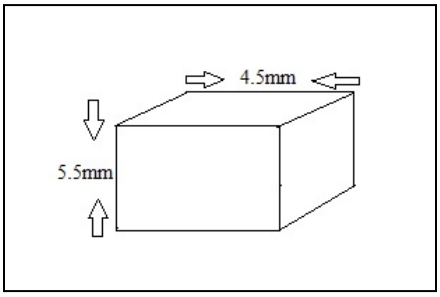


Fig. 3: Size of sample for XRD analysis

Sample Orientation:

If the sample displays a preferred crystallographic orientation, it might be necessary to align it with the X-ray beam in a particular way.

Fig. 4: Picture of XRD machine used for the XRD analysis

To determine the proper orientation for the material of interest, consult relevant literature or crystallographic databases.

To achieve the desired orientation, use the specialized goniometers or alignment stages that the XRD instrument provides.

Once the samples are ready, mount them onto the sample holder or stage of the XRD instrument, making sure they are properly aligned and oriented. Start the analysis after configuring the XRD instrument with the required measurement parameters, such as the copper beam used, whose wavelength was 1.5406 Å, scanning range of 10°-100° and the scanning rate of 2 degrees/min. The crystal structure, phase composition, and other pertinent details of the material can then be ascertained from the diffraction patterns obtained from the XRD instrument.

## *7.5 Microhardness Testing*

1 Selection of Specimens:

For microhardness testing, select representative samples of the material of interest.

To accommodate the indenter during testing, make sure the samples are 5 mm in height and 4.5 mm in width.

The polished samples should be submerged in the nital etchant solution for the specified amount of time while following the correct safety procedures and ventilation.

Fig. 5: Conation Digital Vickers Micro Hardness Tester

After etching, carefully rinse the samples with distilled water to halt the etching process and get rid of any leftover etchant. After that, I used diamond indentation with a 100 gf load and a 15 sec dwell time.

## *7.6 Corrosion Test:*

Testing for corrosion is done to determine how susceptible a material is to degrading in corrosive environments. The purpose of the test is to assess the material's corrosion resistance and determine whether it is appropriate for a given application. The procedure for conducting corrosion tests is generally described as follows:

Test Setup:

Set up the corrosion test apparatus or tools in accordance with the test method you've chosen. This may entail setting up an electrochemical cell for electrochemical testing, putting the samples in a test chamber, or submerging them in an acidic solution.


Fig. 6: AUTOLAB corrosion testing machine

Exposure to a Corrosive Environment:

As per the specified test conditions, expose the prepared samples to a corrosive environment, like 3.5 ml of NaCl solution. The samples might then be exposed to a particular corrosive solution, misted with corrosive liquid, or given a particular electrical potential for electrochemical testing.

Throughout the exposure period, keep an eye on the samples to spot any outward indications of corrosion, such as alterations in appearance or colour or the development of corrosion products.

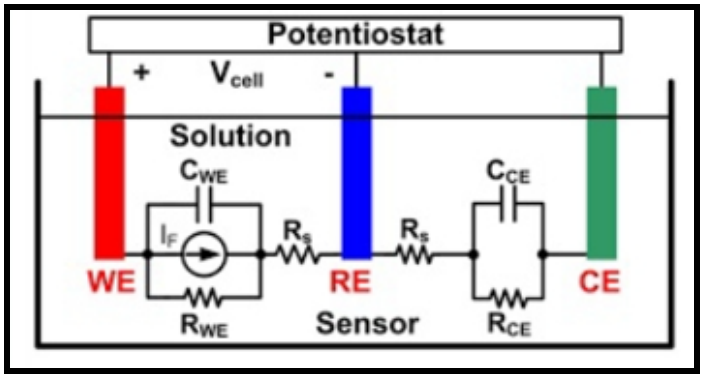


Fig. 7: Circuit of the Corrosion Test

For the corrosion test, I used this circuit, where WE is a rail steel sample used as the working electrode, RE is a saturated calomel electrode used as a reference electrode, and CE is graphite used as a counter electrode.

## 3 Evaluation and Analysis:

Remove the samples from the test environment after the allotted exposure time has passed, and then carefully look for corrosion damage. Keep track of any noticeable alterations in the samples' appearance, surface morphology, or corrosion products. Measure corrosion rates, evaluate pitting or crevice corrosion, examine the metal metallurgically, or analyze the corrosion products using microscopy, spectroscopy, or electrochemical methods, among other additional analyses. It's crucial to remember that the particular test procedure, test setup, and analysis methods may change depending on the kind of corrosion being examined and the demands of the particular application. The process of corrosion testing is generally explained in this outline.

### *7.7 Microstructure observation using a scanning electron microscope (SEM):*

A metallurgical microscope with accessories for image analysis was used for the scanning electron microscopic investigation of the rail steel samples. The SEM of the model number is HITACHI SU 3800 . The applied voltage is 20Kv for this experiment.

The specimens for the test were metallographically polished and etched before a microscopic examination was performed. The polished samples were etched in nital enchant solution. Collect the necessary material for etching before doing the SEM analysis. Magnification 250x, 500x, 1000x, 1500x and 2000x are used in the scanning electron microscope for all samples.


Fig 8: HITACHI scanning electron microscope

# 8 Results and Discussion

## *8.1 Chemical composition of the received rail steel:*

| Items | Quantity (%) |
|---|---|
| C | 0.67 |
| Si | 0.16 |
| S | 0.01 |
| P | 0.01 |
| Mn | 1.10 |
| Ni | <0.001 |
| Cr | 0.01 |
| Mo | 0.002 |
| V | <0.001 |
| Cu | 0.009 |
| Al | 0.002 |
| Sn | 0.005 |
| Sb | 0.003 |
| As | 0.007 |
| B | <0.0001 |
| Nb | 0.008 |
| Ti | <0.001 |
| Co | 0.007 |
| W | 0.022 |
| Zr | 0.01 |

Table 1: Table 1 represents the chemical compositions of the as received rail steel sample

From Table 1, it can be observed that all the chemical components are listed with their amounts in percentage. In this rail, carbon, silicon, sulfur, phosphorus, and manganese are present at 0.67%, 0.16%, 0.01%, 0.01%, and 1.10%, respectively.

## *8.2 Microstructure of base material substrate and heat-treated rail steel samples*

Annealing is a heat-treatment procedure used to change a material's microstructure, usually to enhance its mechanical properties. The particular annealing conditions, such as temperature and holding period, can have an impact on the steel's final microstructure.

High-carbon steel is typically alloyed with other elements to increase its strength, toughness, and wear resistance in rail steel. Rail steel has a variety of microstructures, including ferrite, pearlite, and occasionally bainite or martensite, depending on the composition of the alloy and heat treatment.

From Fig. 9, it can be observed that 0.6% carbon steel is a type of medium carbon steel that contains approximately 0.6% carbon by weight. The microstructure of this steel is primarily composed of ferrite and cementite.

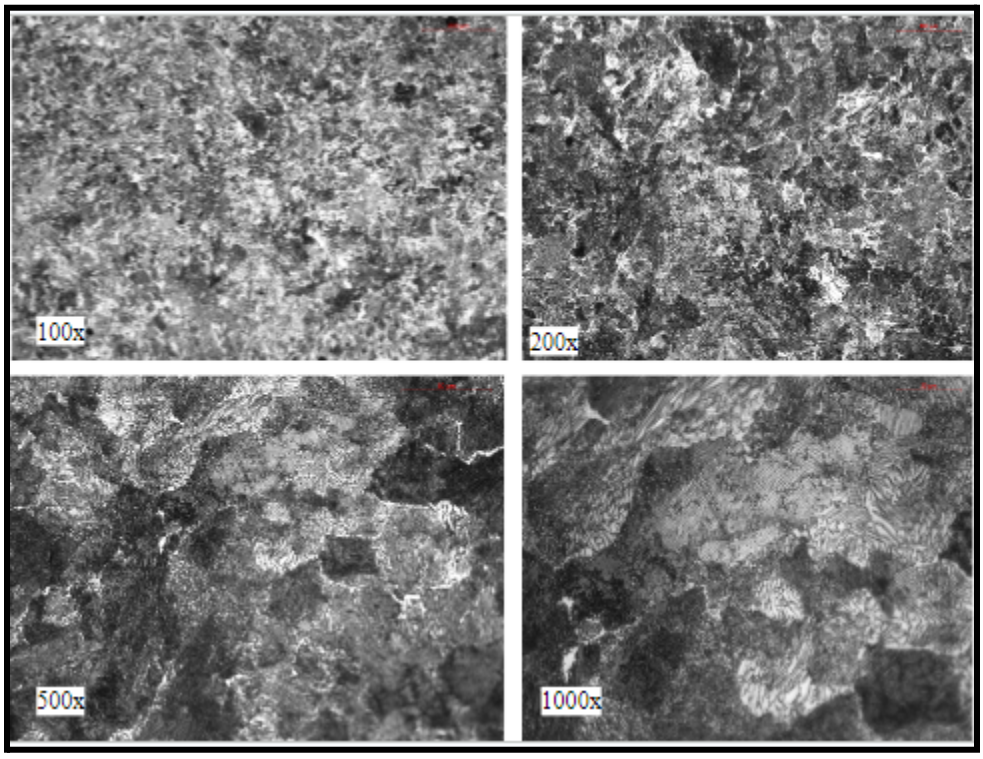


Figure 9: Microstructure of base sample

The rail steel would be heated above its critical temperature, changing the microstructure into pearlite, at an annealing temperature of 1005°C. The face-centred cubic (FCC) crystal structure describes the high-temperature phase known as pearlite.

The goal is to maintain a constant temperature throughout the material for the entire 15-minute holding period in order to ensure a uniform transformation of the microstructure. The carbon atoms can diffuse when the steel is kept at this temperature for a long enough time, which helps the formation of the desired microstructural phases.

From Fig. 10, it can be observed that after annealing, the subsequent cooling procedure is essential and can significantly affect the final microstructure. Austenite was changed into ferrite and pearlite.

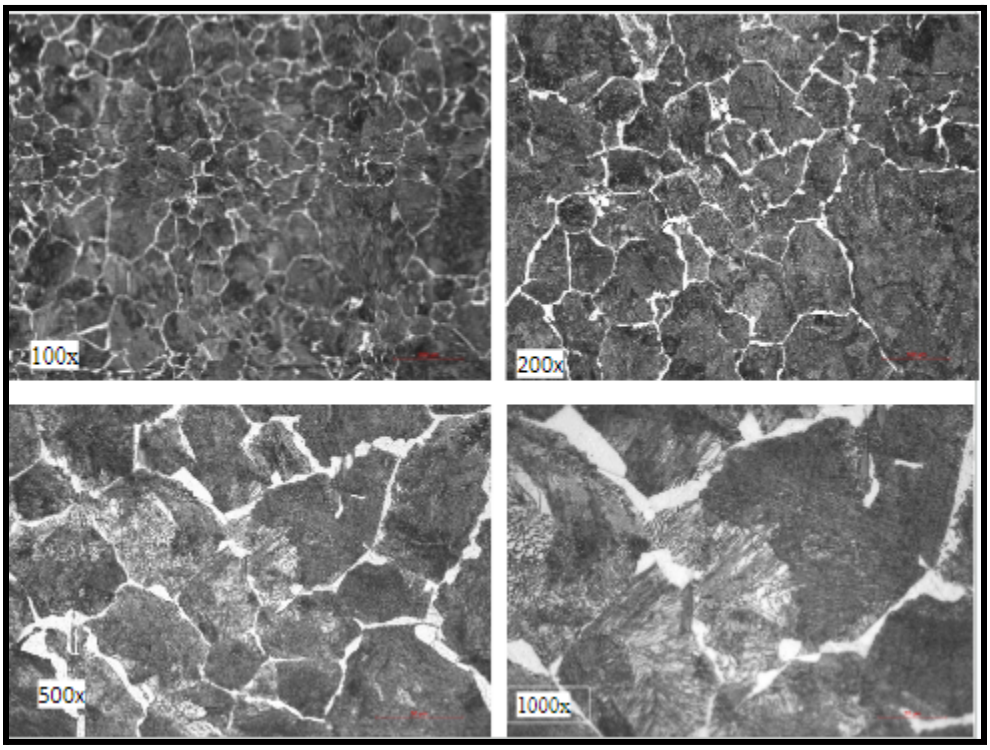


Figure 10: Microstructure of the Sample Heated at 1005 °C

Rail steel is then typically heated above its critical temperature at an annealing temperature of 910°C in order to change its microstructure into austenite, a high-temperature phase with a face-centred cubic (FCC) crystal structure. Austenite allows for carbon diffusion, which is required for upcoming microstructural changes.

The 15-minute holding period is intended to ensure a consistent transformation of the steel. The formation of the desired microstructural phases and carbon diffusion are made possible

during this time period. It is important to remember that both the composition of the steel and the rate of cooling after annealing affect the distribution and specific microstructural elements of rail steel.

From Fig. 11, it can be observed that the subsequent cooling process from the annealing temperature is crucial and capable of significantly affecting the final microstructure. The transformation of austenite into different phases like ferrite, pearlite, bainite, or martensite depends on the rate of cooling.

Because of the annealing with a 15-minute holding time and slow cooling rate, coarse pearlite, which is made up of alternating layers of ferrite and cementite, is encouraged to form. Pearlite which is coarser has a lower hardness but better toughness.

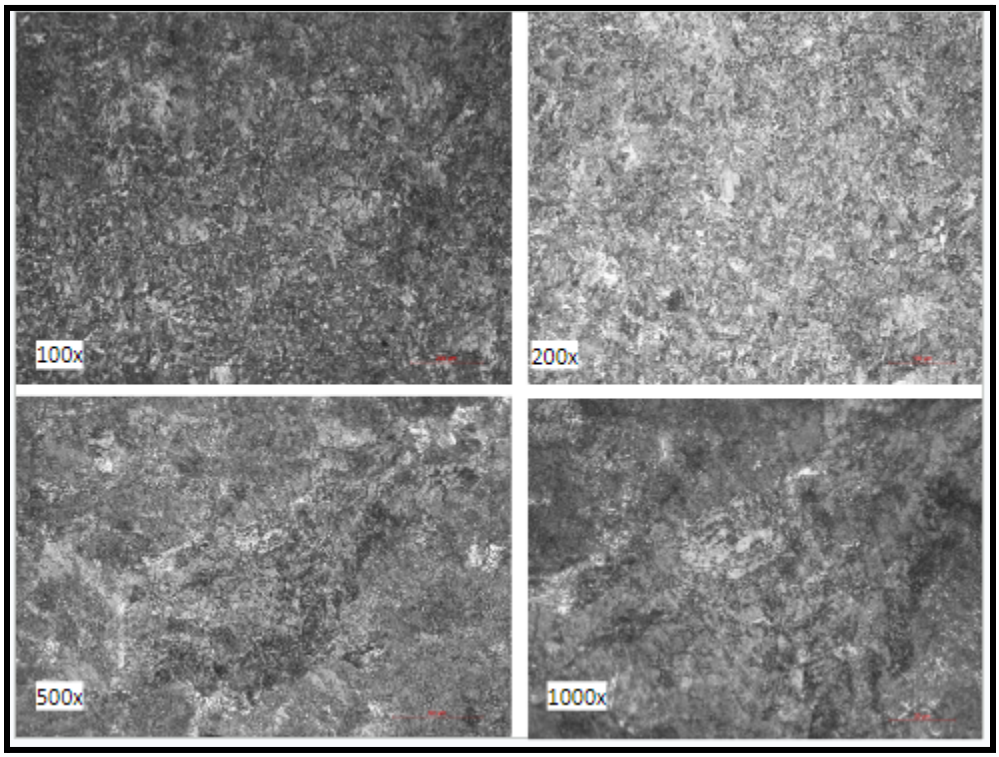


Figure 11: Microstructure of the Sample Heated at 910 °C

Rail steel would typically be heated above its critical temperature at an annealing temperature of 810°C to transform the microstructure into austenite. Austenite has a face-centred cubic (FCC) crystal structure and is a high-temperature phase.

The goal of the 15-minute holding time is to allow for a uniform transformation of the microstructure throughout the rail steel. This duration allows for carbon diffusion and the

formation of desired microstructural phases. However, the specific microstructural constituents and their distribution would be determined by the composition of the rail steel and the cooling rate used after annealing.

From Fig. 12, it can be observed that the cooling rate is slow during annealing, and pearlite, which is made up of a fine lamellar pearlitiv structure consisting of alternate ferrite and cementite phase. Pearlite has a good strength-to-toughness ratio.

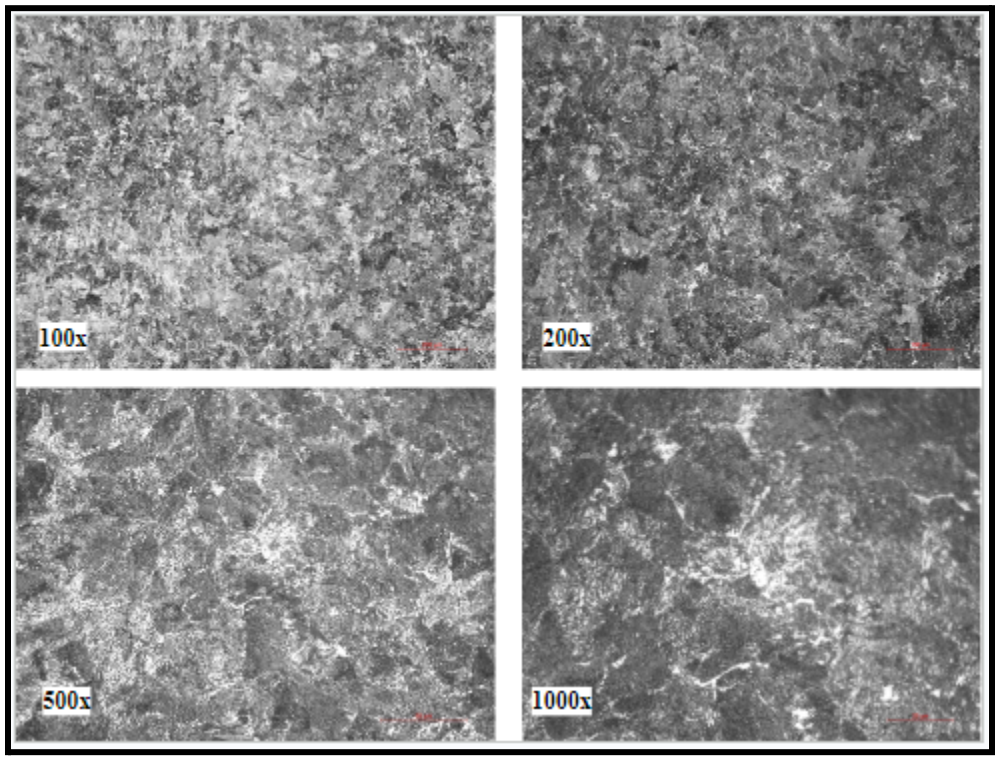


Figure 12: Microstructure of the Sample Heated at 810 °C

From Fig. 13, it can be observed that at an annealing temperature of 705°C, rail steel would typically be heated above its critical temperature to transform the microstructure into austenite. Austenite is a high-temperature phase with a face-centred cubic (FCC) crystal structure.

During the 15-minute holding time, the purpose is to allow for a homogeneous transformation of the microstructure throughout the rail steel. This duration enables carbon diffusion and facilitates the formation of desired microstructural phases. However, the specific microstructural constituents and their distribution would depend on the rail steel's composition and the cooling rate employed after annealing.

From Fig. 13, it can be observed that when the cooling rate is slow during annealing, it promotes the formation of pearlite, which is made up of spheroidization of the pearlite phase as compared to Ref[10]. Pearlite has a good balance of strength and toughness.

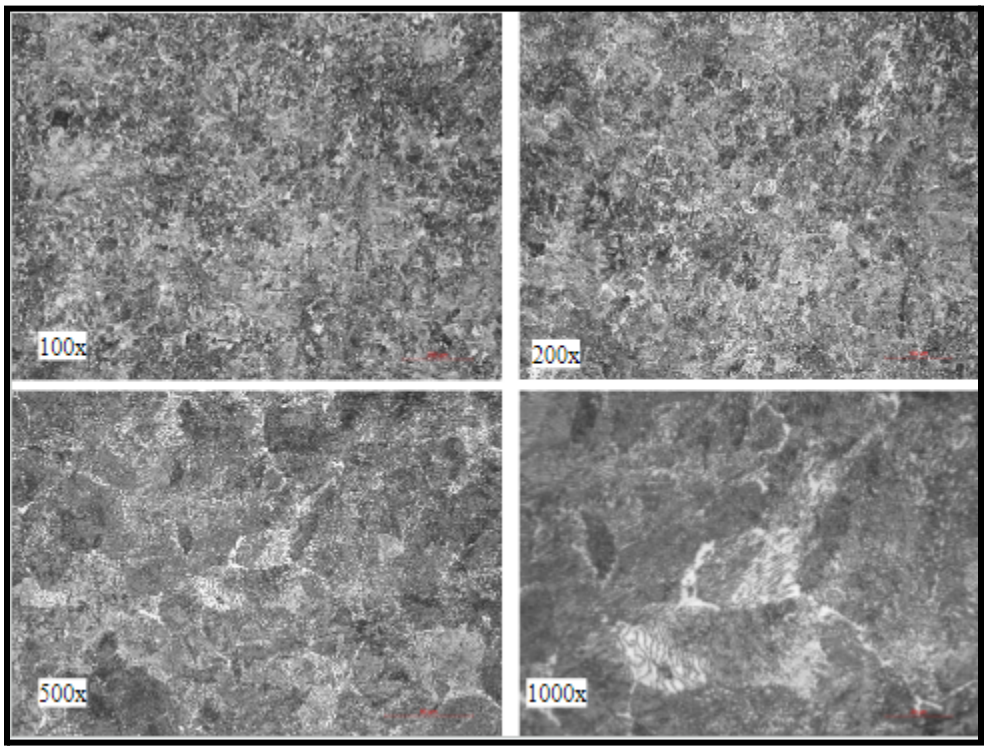


Figure 13: Microstructure of the Sample Heated at 705 °C

### *8.3 Scanning electron microscope of the base material substrate and heat-treated rail steel samples:*

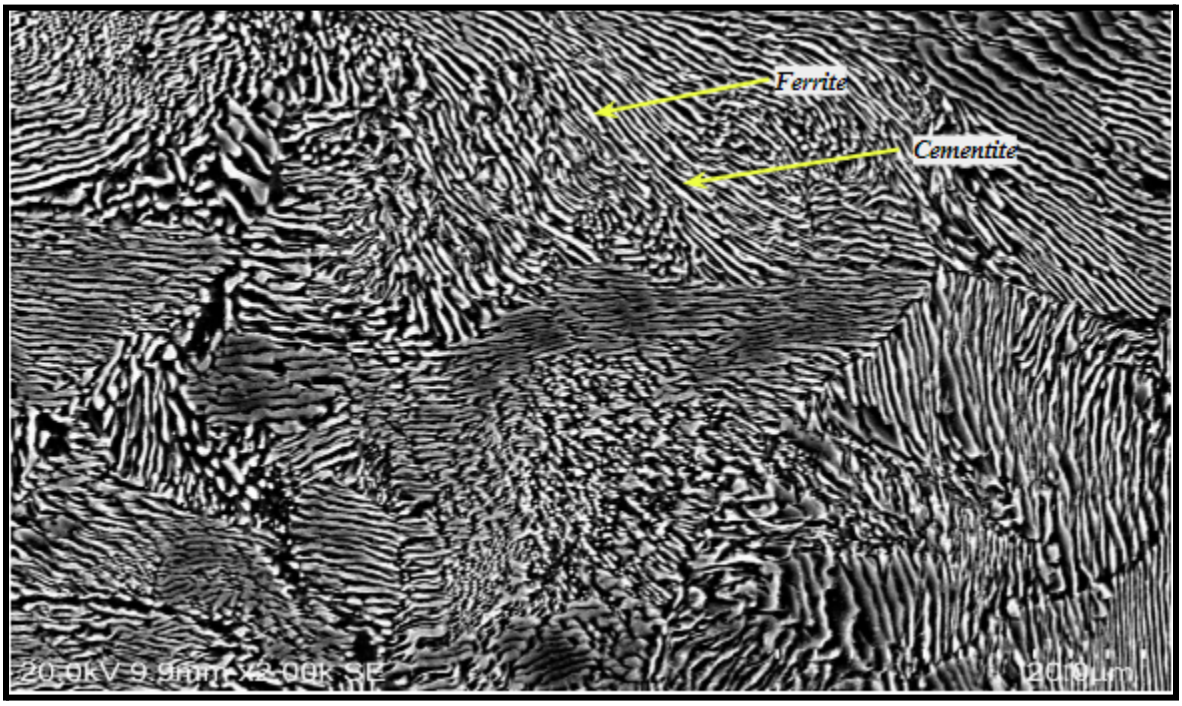


Fig. 20: Microstructure of the base sample with 2000x magnification

From Fig. 20, it has been observed with 2000x magnification that 100% pearlite is present in the microstructure. The white phase indicates the ferrite phase and the black phase indicates the cementite phase. It has also been clearly observed a presence of pearlite colony in the microstructure. The orientation of the pearlite phases is different in each grain body and the grain boundary between the two grains is also clearly observed from the microstructure of the base sample.

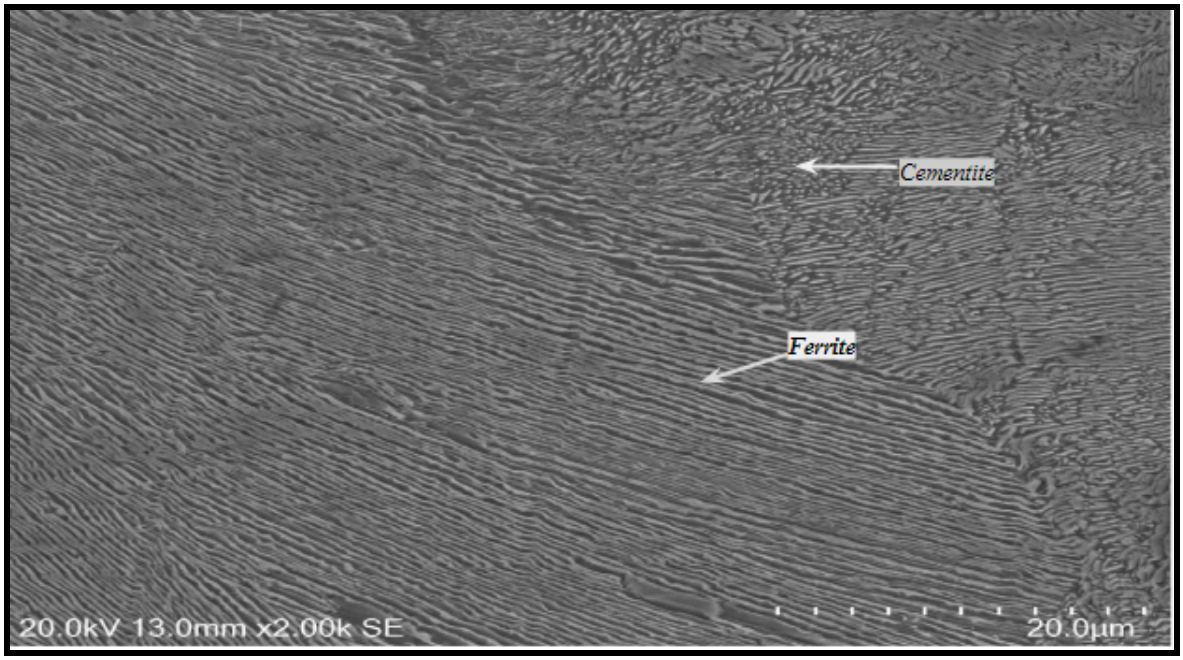


Fig. 21: Microstructure of the Heat-treated sample at 1005 °C with 2000x magnification

From Fig. 21, it has been observed with 20000x magnification that 100% pearlite is present in the microstructure. The white phase indicates the ferrite phase and the black phase indicates the cementite phase. It has also been clearly observed a presence of pearlite colonies in the microstructure but the number of pearlite colonies is less with compared to the base sample. Also, the annealed temperature increases grain refinement occurs and stress relief also occurs. The orientation of the pearlite phases is different in each grain body and the grain boundary between the two grains is also clearly observed from the microstructure of the heat-treated(annealed) sample at 1005 °C.

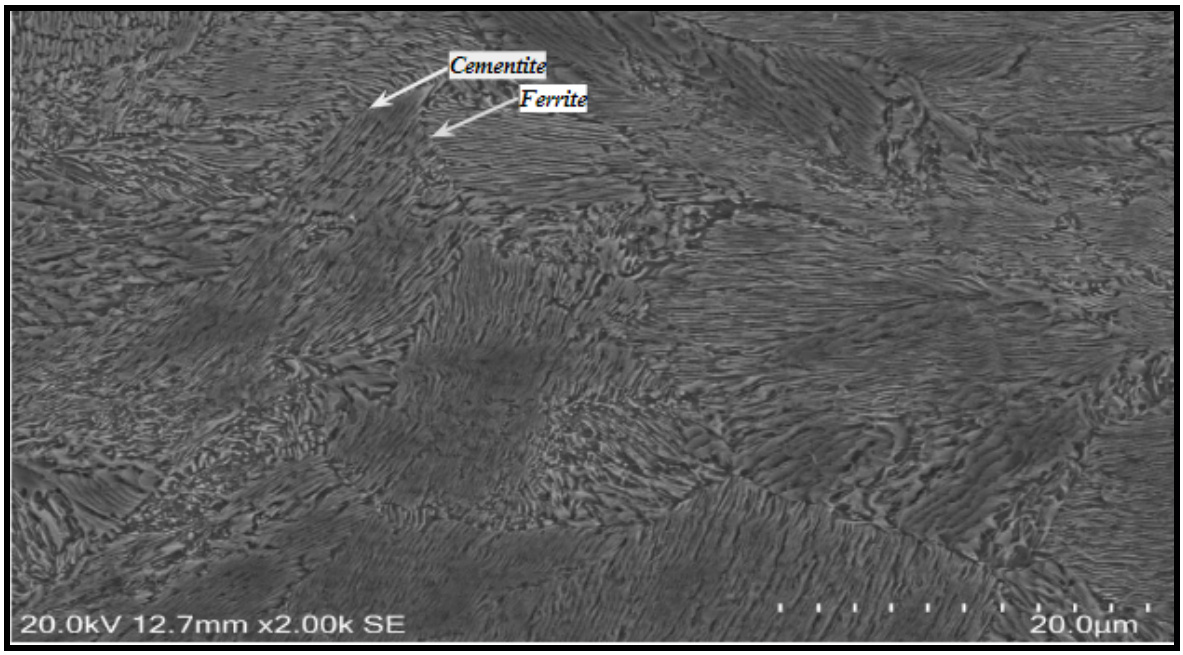


Fig. 22: Microstructure of the Heat-treated sample at 910 °C with 2000x magnification

From Fig. 22, it can be observed with 20000x magnification that pearlite is present in the microstructure. The white phase indicates the ferrite phase and the black phase indicates the cementite phase. It has also been clearly observed a presence of pearlite colonies in the microstructure but the number of pearlite colonies is less with compared to the base sample but greater than the Heat-treated(annealed) sample at 1005 °C. In this sample annealed temperature increases grain refinement occurs and stress relief also occurs which is less than the heat-treated(annealed) sample at 1005 °C. The orientation of the pearlite phases is different in each grain body and the grain boundary between the two grains is also clearly observed from the microstructure of the heat-treated(annealed) sample at 910 °C.

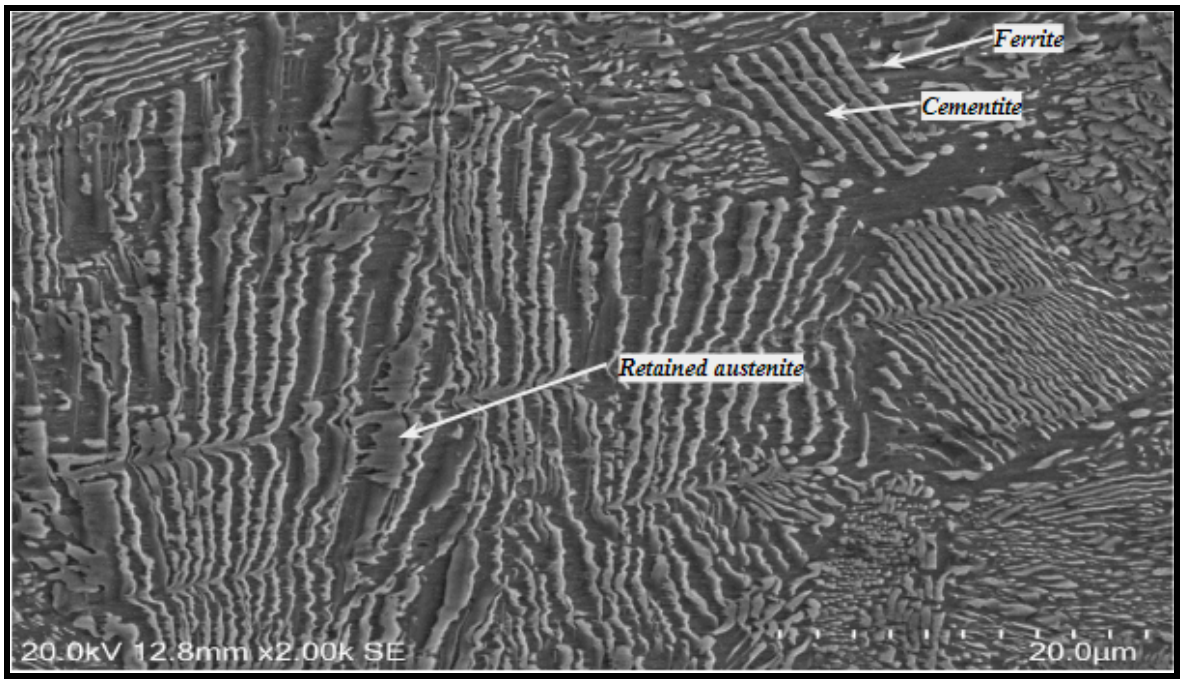


Fig. 23: Microstructure of the Heat-treated sample at 810 °C with 2000x magnification

From Fig. 23, it can be observed with 20000x magnification that pearlite is present in the microstructure. The white phase indicates the ferrite phase and the black phase indicates the cementite phase. But in this microstructure, retained austenite was present. It has also been clearly observed a presence of pearlite colonies in the microstructure but the number of pearlite colonies is less with compared to the base sample but greater than the Heat-treated(annealed) samples at 1005 °C and 910 °C. The orientation of the pearlite phases is different in each grain body and the grain boundary between the two grains is not clearly observed from the microstructure of the Heat-treated (annealed) sample at 810 °C.

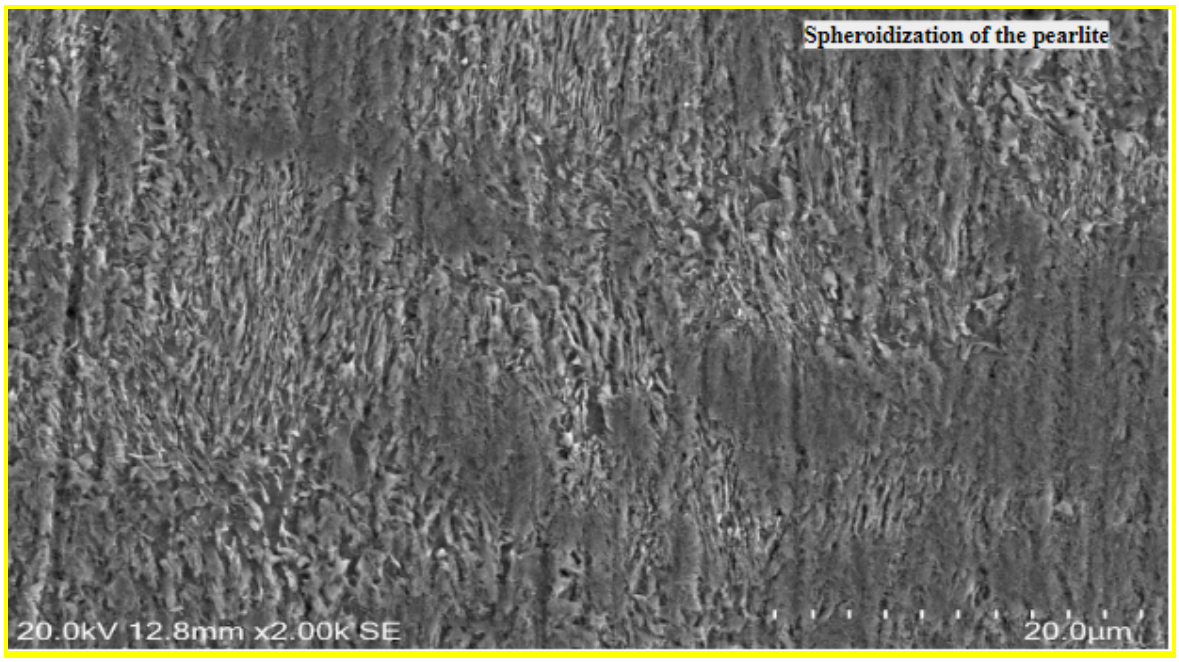


Fig. 24: Microstructure of the Heat treated sample at 705 °C with 2000x magnification

From Fig. 24, it can be observed with 20000x magnification that only spheroidization of the pearlite phase is present in the heat-treated sample by the annealing method at 705 °C. This microstructure is characterized by the transformation of the lamellar pearlite into a microstructure with rounded or spheroidal cementite particles dispersed within the ferrite matrix. The cementite particles were originally present in the form of lamellae as compared to Ref [11].

## *8.4 Energy dispersive spectroscopy (EDS) of base material:*

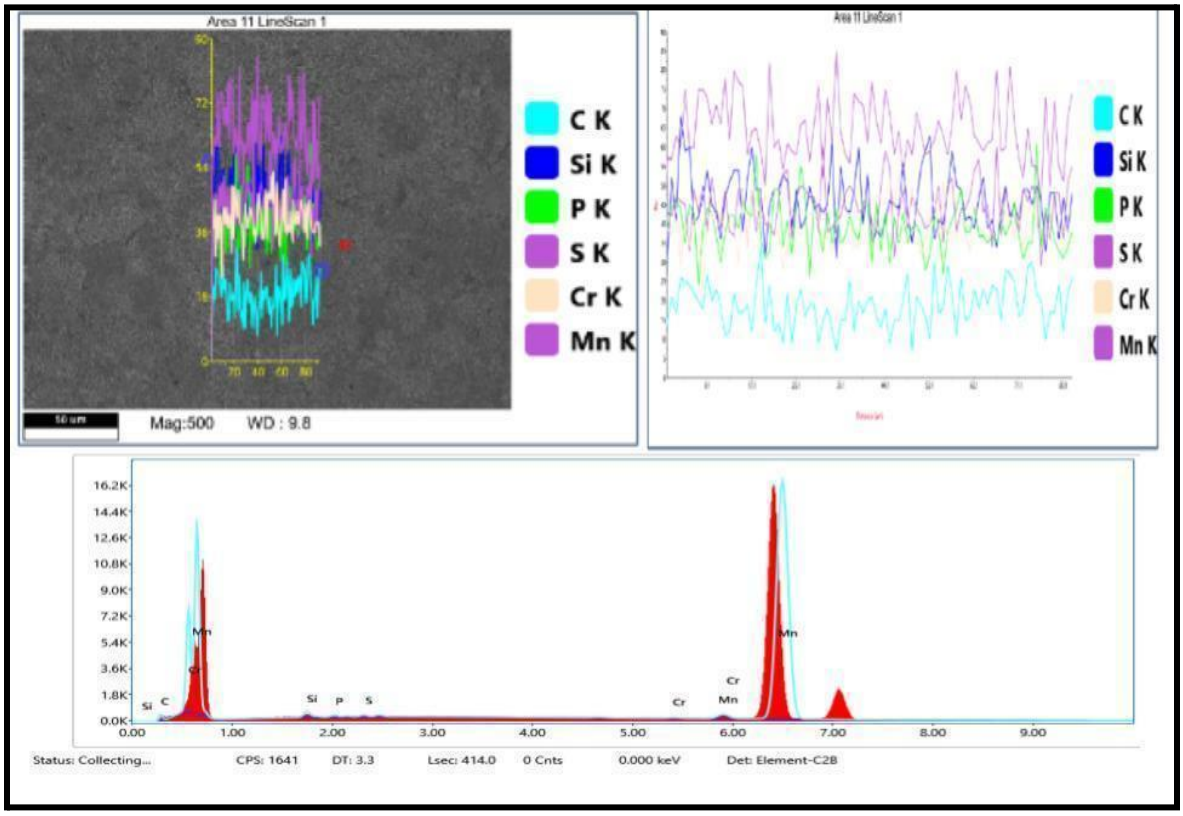


Fig. 25: Results of Energy dispersive spectroscopy (EDS) of base material

| Element | Weight % | Atomic % | Error % | Net Int. | R | A | F |
|---|---|---|---|---|---|---|---|
| | | | | | | | |
| **C K** | 67.80 | 87.55 | 14.82 | 4.26 | 0.9079 | 0.0247 | 1 |
| **Si K** | 7.17 | 3.95 | 10.92 | 8.25 | 0.9403 | 0.4131 | 1.0110 |
| **P K** | 3.45 | 1.73 | 18.45 | 3.24 | 0.9433 | 0.4483 | 1.0136 |
| **S K** | 3.09 | 1.50 | 15.08 | 3.27 | 0.9462 | 0.5238 | 1.0157 |
| **Cr K** | 2.91 | 0.87 | 33.34 | 2.13 | 0.9658 | 0.9354 | 1.0713 |
| **Mn K** | 15.58 | 4.40 | 2.23 | 9.67 | 0.9680 | 0.9486 | 1.0376 |

Table 3: The elemental composition of base sample

### *8.5 Microhardness of the base material substrate and heat-treated rail steel samples:*

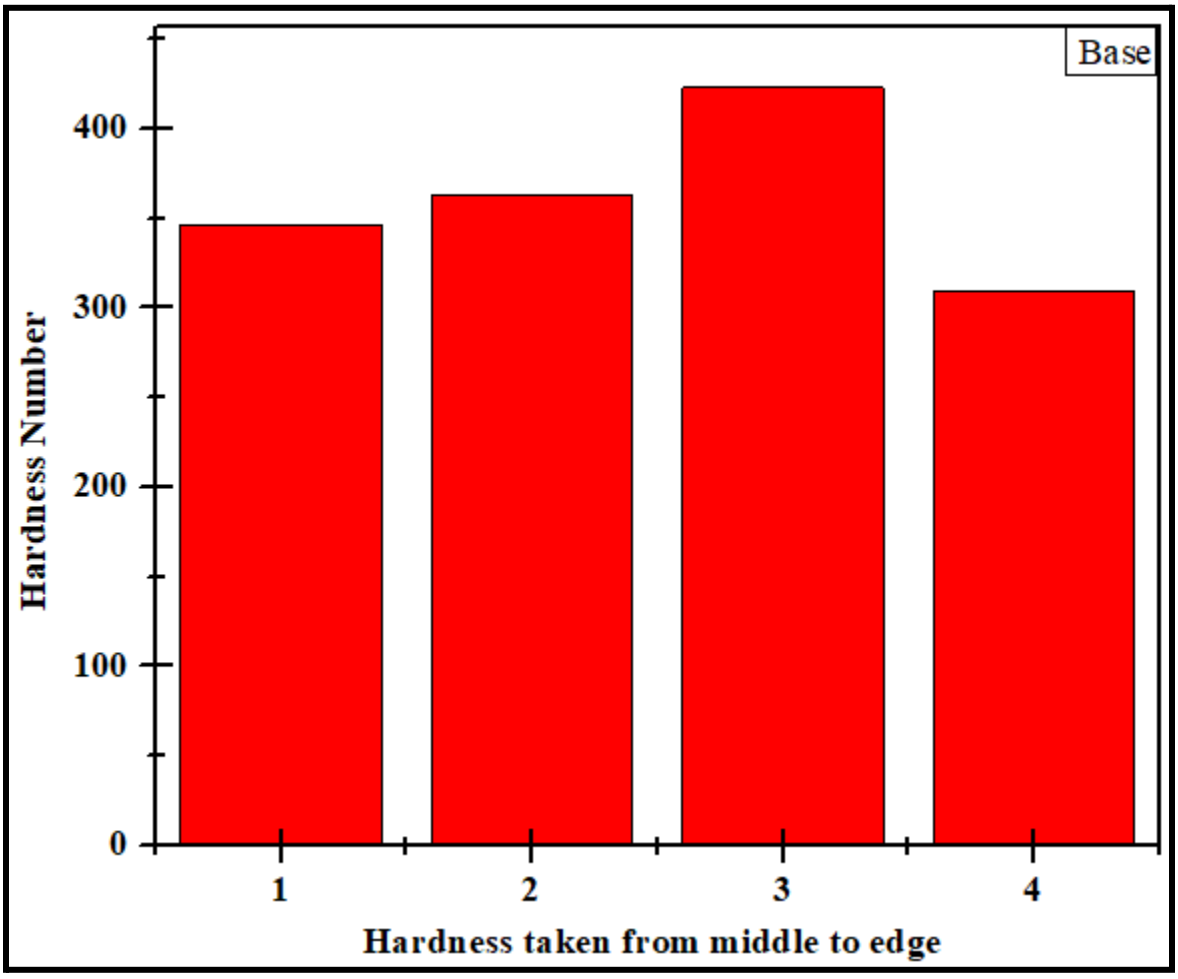


Fig. 14: Microhardness of the Base Sample

From Fig. 14, it can be observed that the hardness of the received sample of rail steel. There are four hardnesses taken from the middle to the edge area. Fig. 13 represents the four hardness numbers: 346.6 Hv, 362.9 Hv, 422.9 Hv and 308.8 Hv respectively. The average hardness of the base sample is 219.675± Hv.

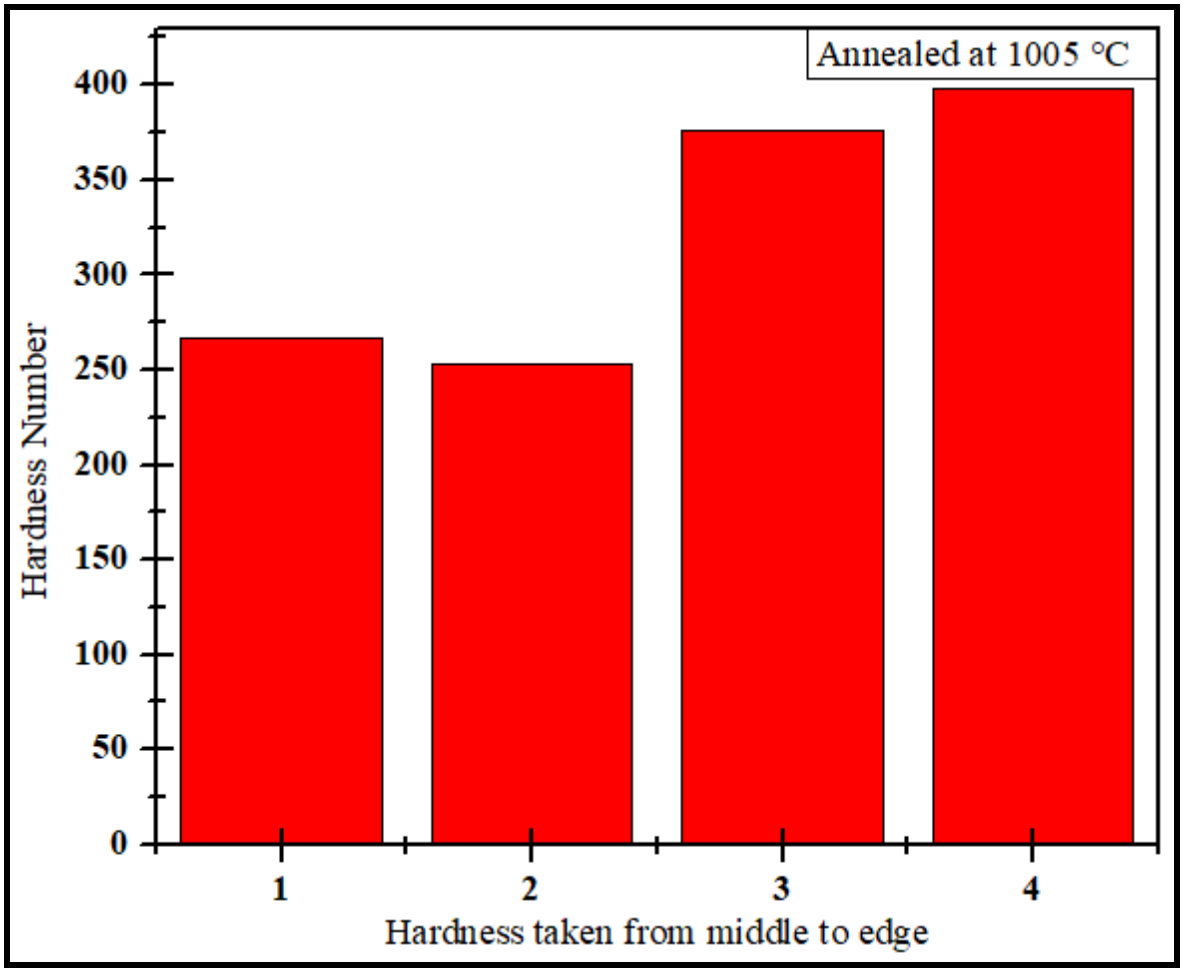


Fig. 15: Microhardness of the Sample Heated at 1005 °C

From Fig. 15, it can be observed that the hardness of the heat-treated sample of rail steel at 1005 °C. There are four hardnesses taken from the middle to the edge area. In Fig. 14, the four hardness numbers are 267.2 Hv, 253.3 Hv, 397.6 Hv, and 376.1 Hv respectively. After the heat treatment, it shows that the edge area has more hardness than the middle area. The average hardness of the sample heated at 1005 °C is 323.55± Hv.

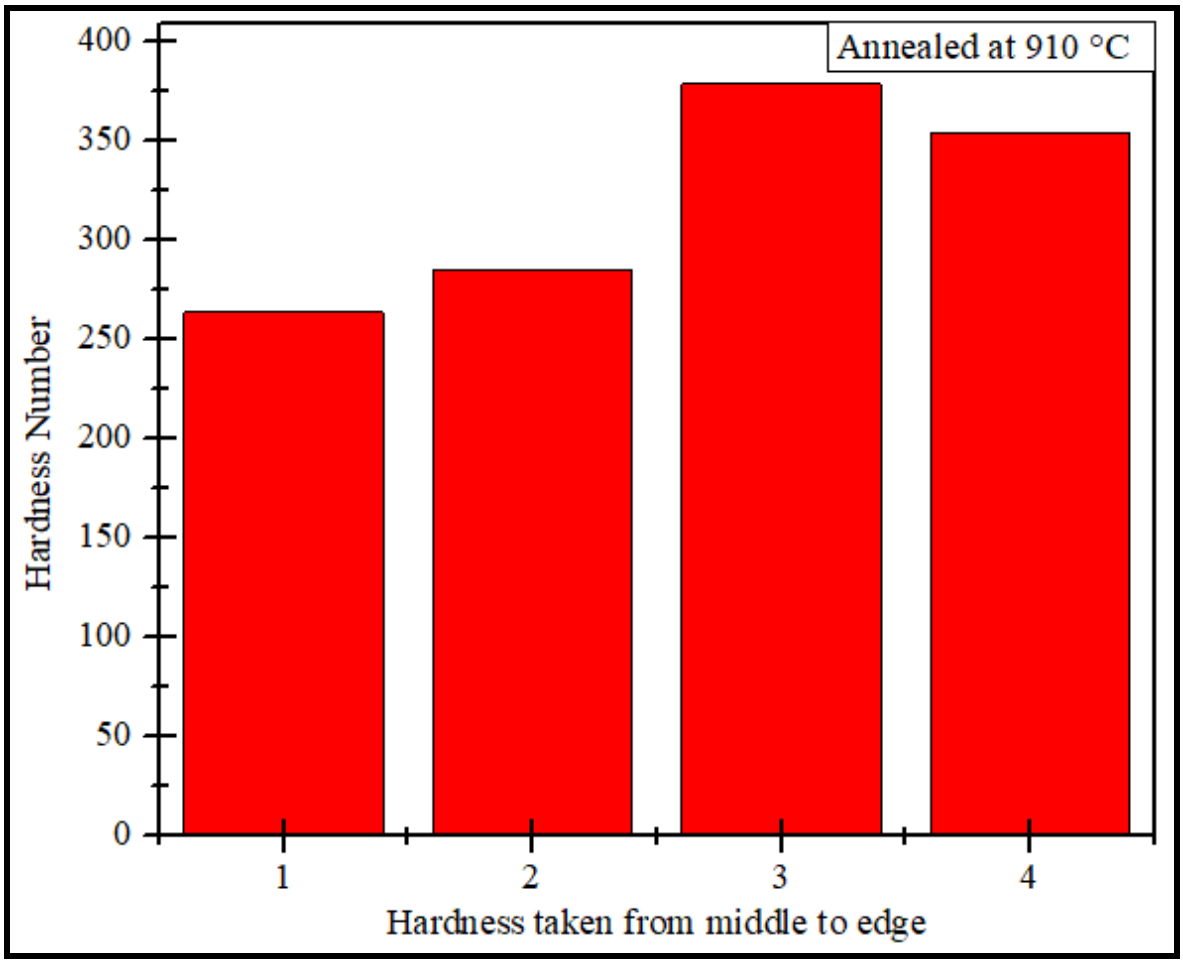


Fig. 16: Microhardness of the Sample Heated at 910 °C

From Fig. 16, it can be observed that the hardness of the heat treat sample of rail steel was 910°C. There are four hardnesses taken from the middle to the edge area. Fig. 15 represents the four hardness numbers that are 263.3 Hv, 285.2 Hv, 378.3 Hv, and 353.5 Hv respectively. After the heat treatment, it shows that the edge area has more hardness than the middle area. The average hardness of the sample heated at 910 °C is 320.075± Hv.

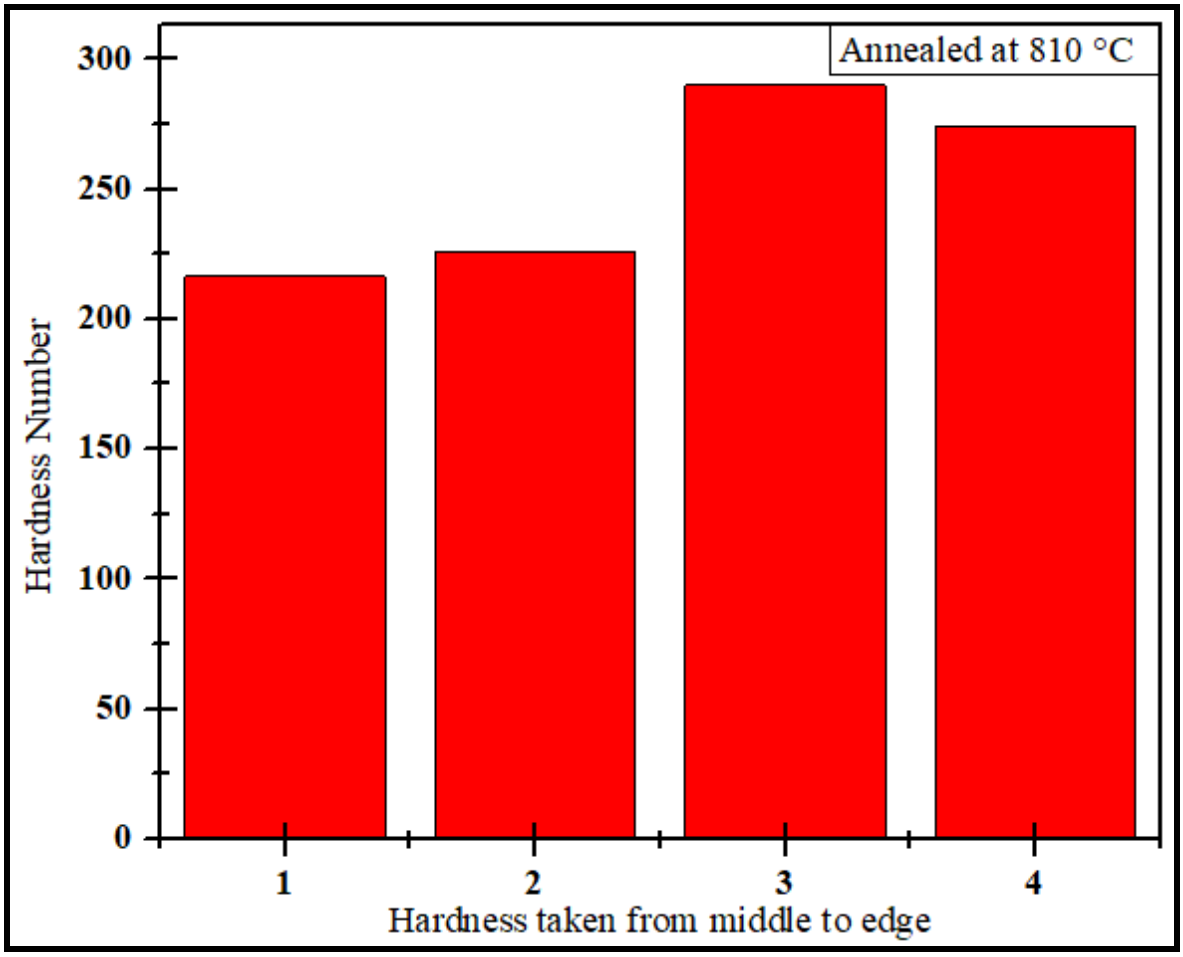


Fig. 17: Microhardness of the Sample Heated at 810 °C

From Fig. 17, it can be observed that the hardness of the heat treat sample of rail steel was 810 °C. There are four hardnesses taken from the middle to the edge area. Fig. 17 represents the four hardness numbers: 216.3 Hv, 226 Hv, 289.9 Hv and 274 Hv. After the heat treatment, it appears that the edge area has more hardness than the middle area. The average hardness of the sample heated at 810 °C is 251.55± Hv.

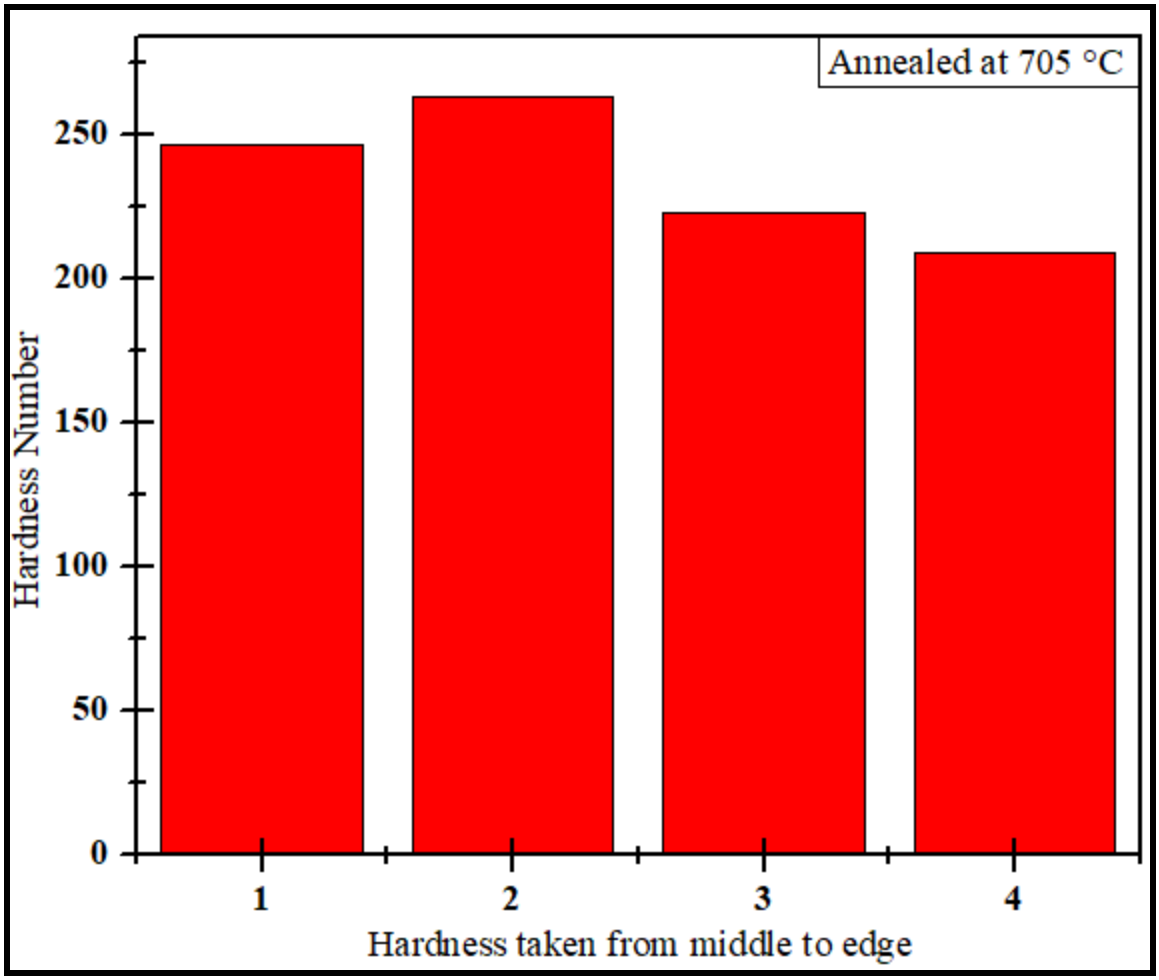


Fig. 18: Microhardness of the Sample Heated at 705 °C

From Fig. 18, it can be observed that the hardness of the heat treat sample of rail steel was 705°C. There are four hardness numbers taken from the middle to the edge area. Fig. 18, represents the four hardness numbers that are 246.6 Hv, 262.9 Hv, 222.9 Hv, and 208.8 Hv, respectively. After the heat treatment, it shows that the middle area has more hardness than the edge area. The average hardness of the sample heated at 705 °C is 235.3± Hv.

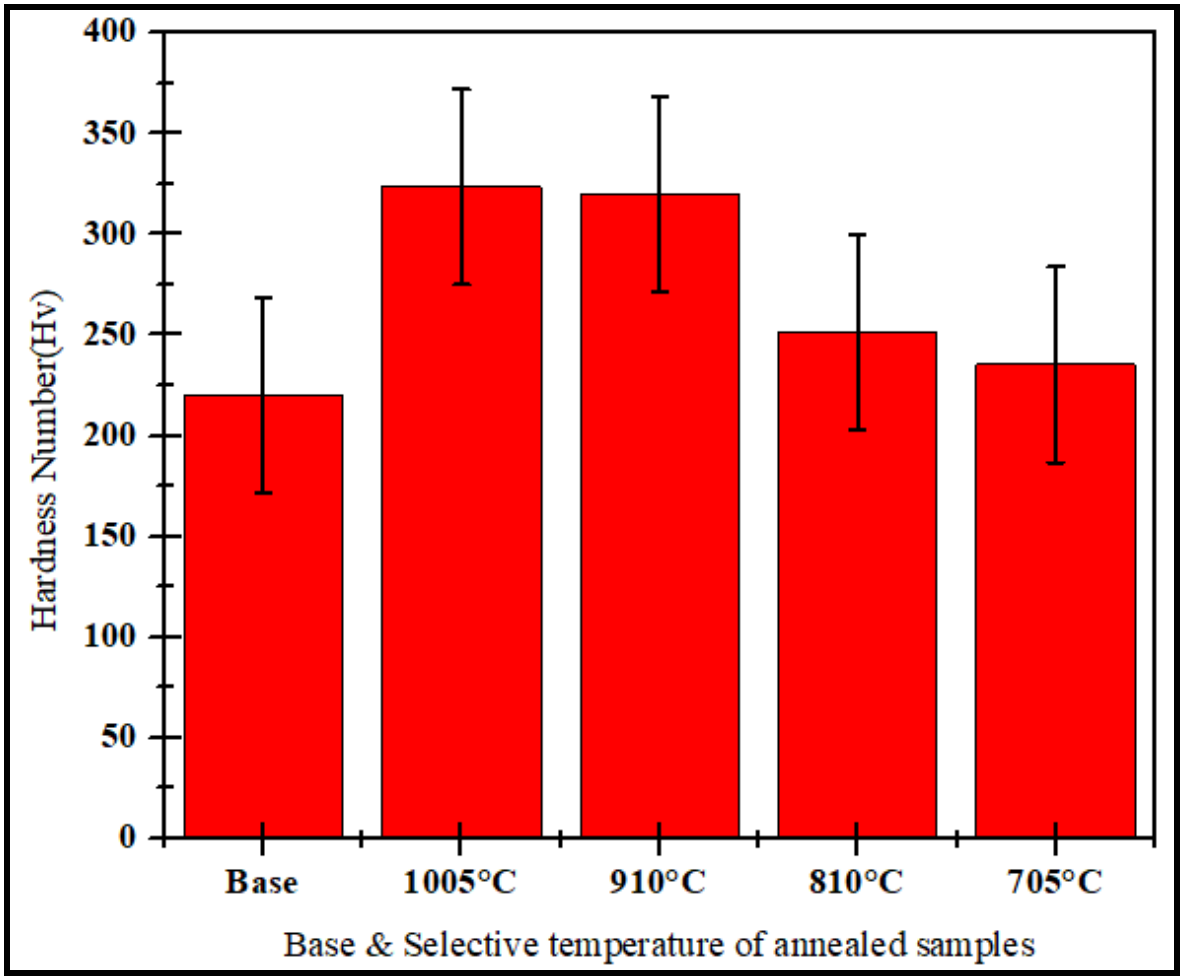


Fig. 19: Average Vicker's microhardness (Hv) of all samples

| Samples of rail steel | Average Vicker's microhardness (Hv) |
|---|---|
| Base | 219.675± |
| 1005°C | 323.55± |
| 910°C | 320.075± |
| 810°C | 251.55± |
| 705°C | 235.3± |

Table 2: Average hardness of all samples

From Fig. 19 and Table 2, it can be revealed that the average Vicker's microhardness (Hv) values of the four heat-treated samples of the rail steel were decreasing with the respect of

decreasing the annealing temperature because decreasing the annealing temperature of rail steel can result in bigger grain sizes, incomplete phase transitions, uneven carbon distribution, residual stresses, and changes in the distribution of alloying elements, all of which can contribute to a fall in Vickers microhardness. The specific effect of lowering the annealing temperature will be determined by the composition of the rail steel and the desired mechanical qualities. Typically, a highly controlled annealing procedure is required to attain the necessary mix of hardness and other mechanical qualities in rail steel.

### *8.6 XRD of the base material substrate and heat-treated rail steel samples:*

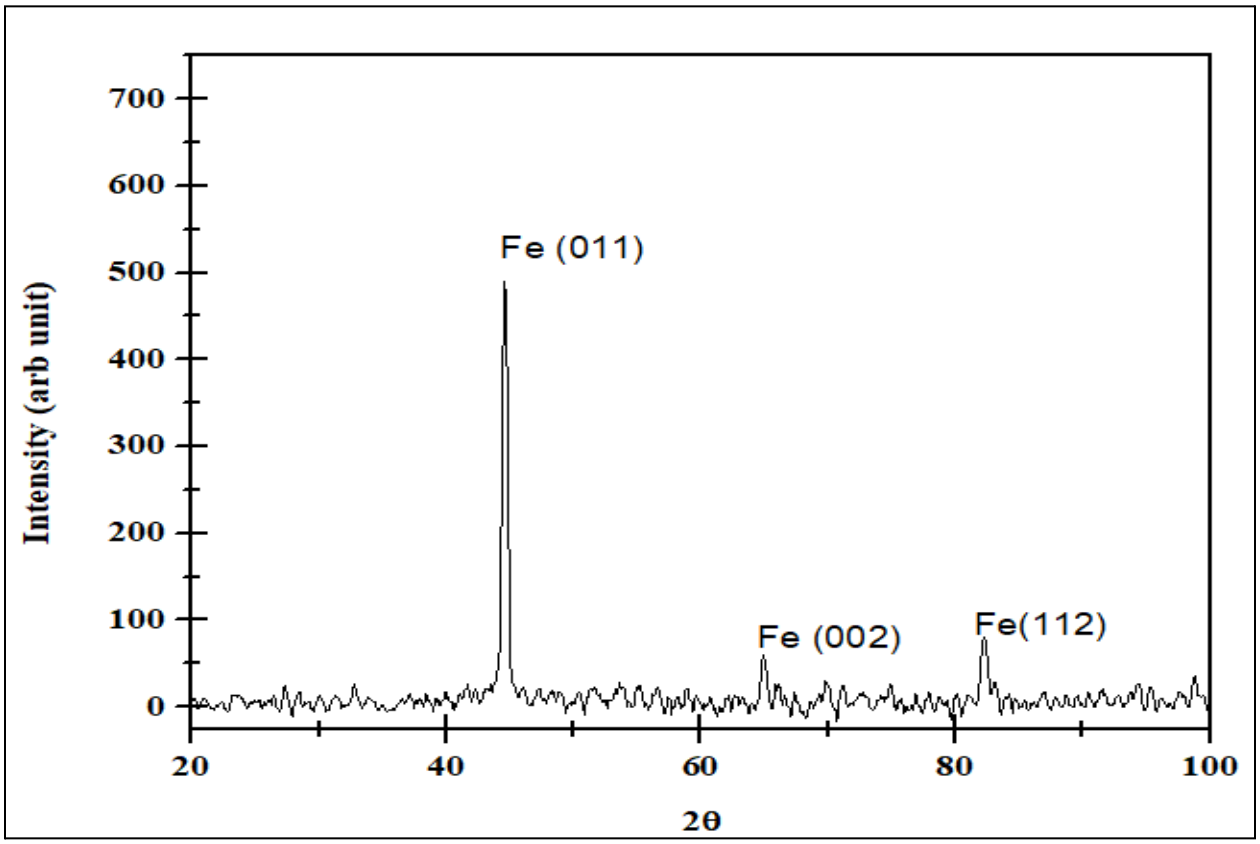


Fig. 26: X-ray diffraction study of the base sample

From Fig. 26, it can be revealed that in the results of the XRD of the base sample, there are three peak finds of Fe, and the planes are (011), (002), and (112). In the first peak Fe(011), the d-spacing (Å) is 2.0722; and the 2θ value is 44.665. The second peak Fe(002), the d-spacing

(Å) is 1.43355; and the 2θ value is 65.005. The third peak is Fe(112); the d-spacing (Å) is 1.17045; and the 2θ value is 82.313.

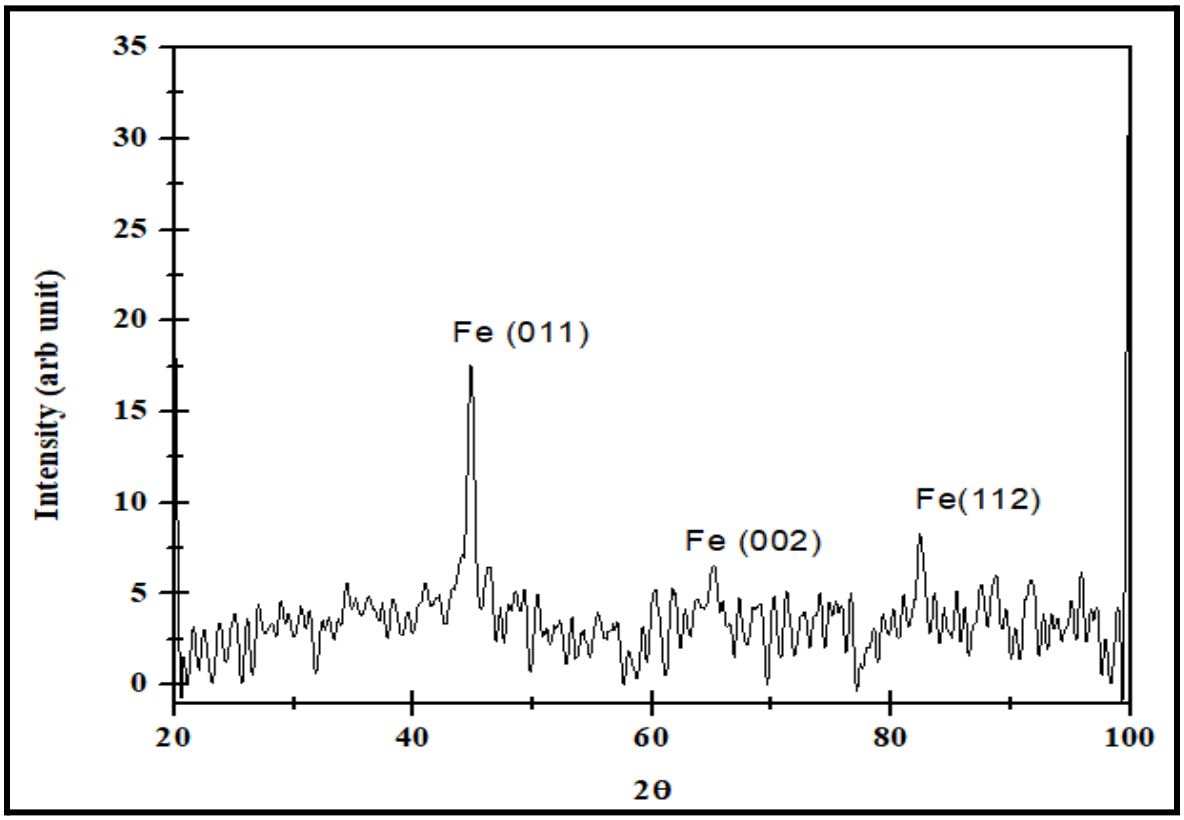


Fig. 27: X-ray diffraction study of the Heat treated sample at 1005 °C

From Fig. 27, it can be revealed that in the results of the XRD of the base sample, there are three peak finds of Fe, and the planes are (011), (002), and (112). In the first peak Fe(011), the d-spacing (Å) is 2.0285; and the 2θ value is 44.636. The second peak Fe(002), the d-spacing (Å) is 1.4334; and the 2θ value is 65.012. The third peak is Fe(112); the d-spacing (Å) is 1.1708; and the 2θ value is 82.280. Also, in this sample, the peak heights are smaller than the base sample.

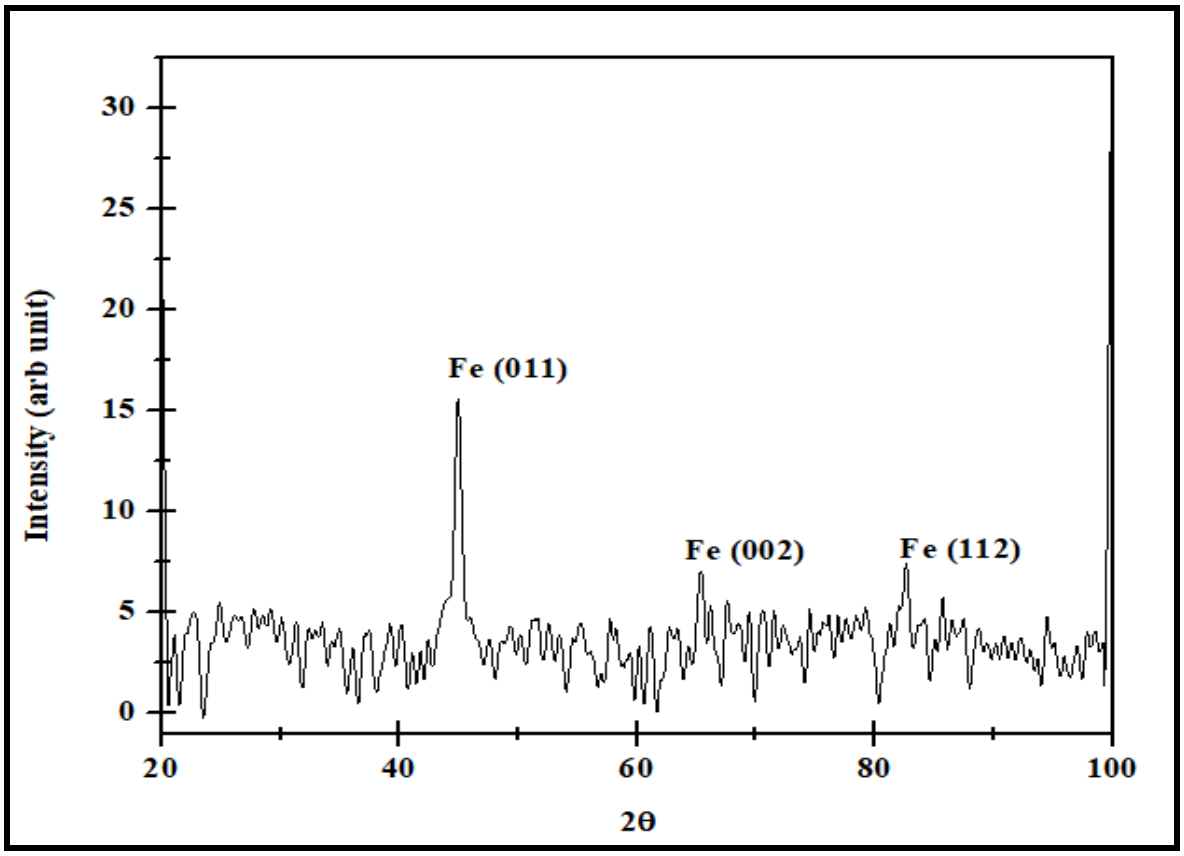


Fig. 28: X-ray diffraction study of the Heat treated sample at 910°C

From Fig. 28, it can be revealed that in the results of the XRD of the base sample, there are three peak finds of Fe, and the planes are (011), (002), and (112). In the first peak Fe(011), the d-spacing (Å) is 2.01614; and the 2θ value is 44.9236. The second peak Fe(002), the d-spacing (Å) is 1.42802; and the 2θ value is 65.2878. The third peak is Fe(112); the d-spacing (Å) is 1.16453; and the 2θ value is 82.8239. Also, in this sample, the peak heights are smaller than in the base sample but closely similar to those in the heat-treated sample at 1005°C.

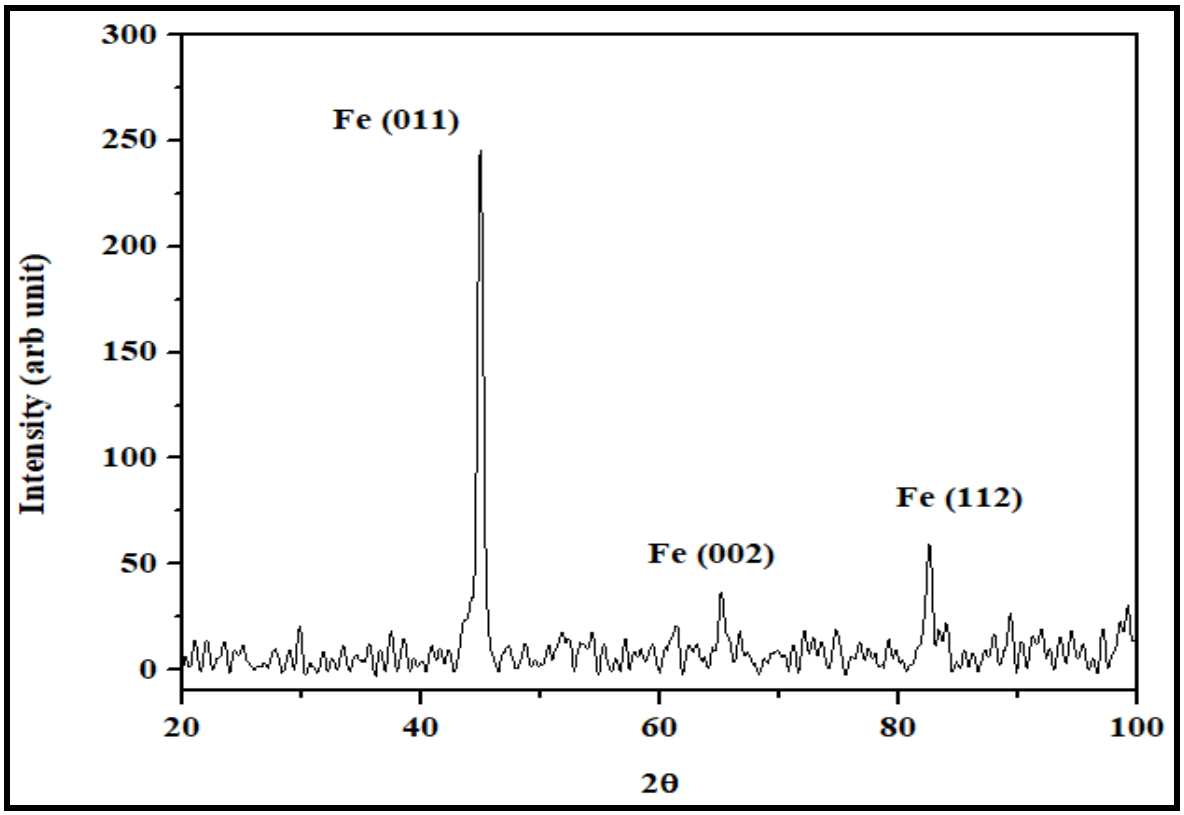


Fig. 29: X-ray diffraction study of the Heat treated sample at 810°C

From Fig. 29, it can be revealed that in the results of the XRD of the base sample, there are three peak finds of Fe, and the planes are (011), (002), and (112). In the first peak Fe(011), the d-spacing (Å) is 2.0162; and the 2θ value is 44.9613. The second peak Fe(002), the d-spacing (Å) is 1.43293; and the 2θ value is 65.0969. The third peak is Fe(112); the d-spacing (Å) is 1.16705; and the 2θ value is 82.68954. Also, in this sample, the peak heights are smaller than in the base sample but greater than in the heat-treated sample at 1005°C and 910°C.

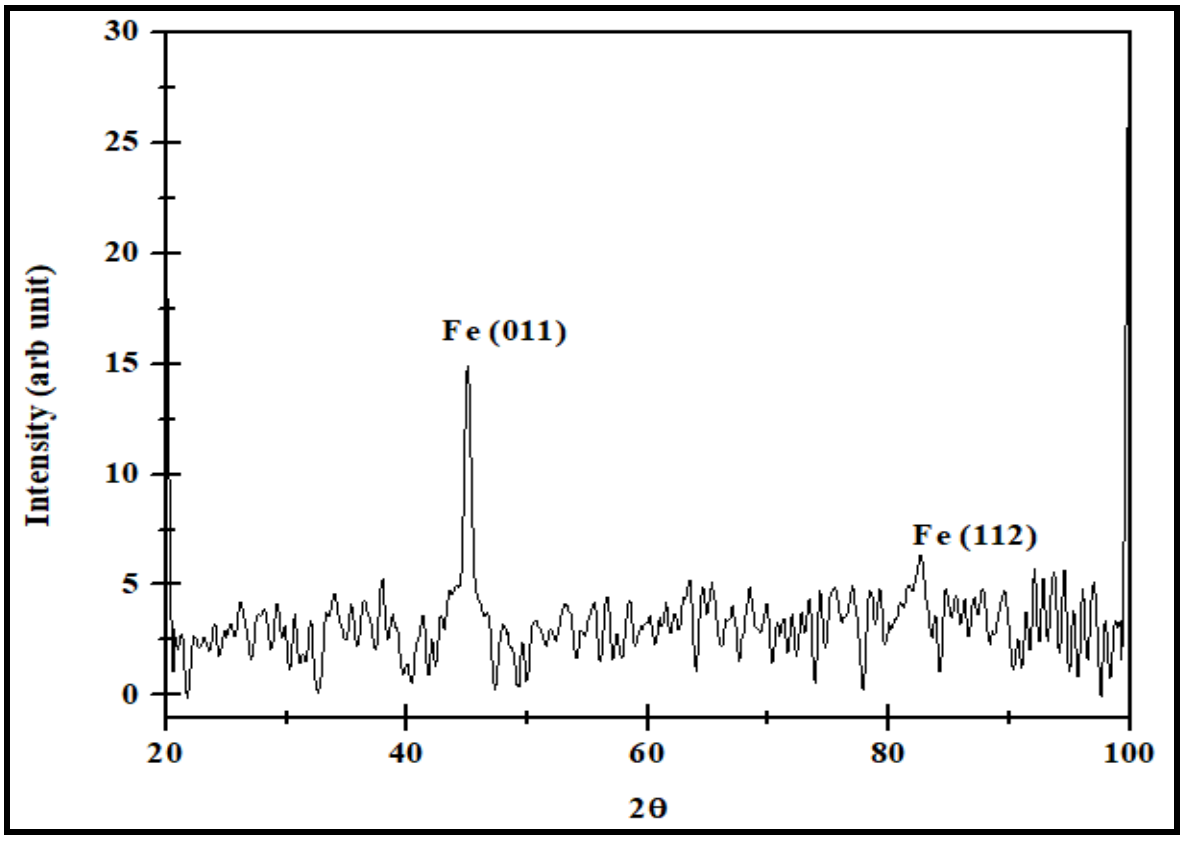


Fig. 30: X-ray diffraction study of the Heat treated sample at 705 °C

From Fig. 30, it can be revealed that in the results of the XRD of the base sample, there are three peak finds of Fe, and the planes are (011), (002), and (112). In the first peak Fe(011), the d-spacing (Å) is 2.01239; and the 2θ value is 45.0510. The second peak Fe(002), the d-spacing (Å) is 1.37003; and the 2θ value is 68.4879. The third peak is Fe(112); the d-spacing (Å) is 1.168; and the 2θ value is 82.6069. Also, in this sample, the peak heights are smaller than in other samples.

## *8.7 Corrosion test of the base material substrate and heat-treated rail steel samples*

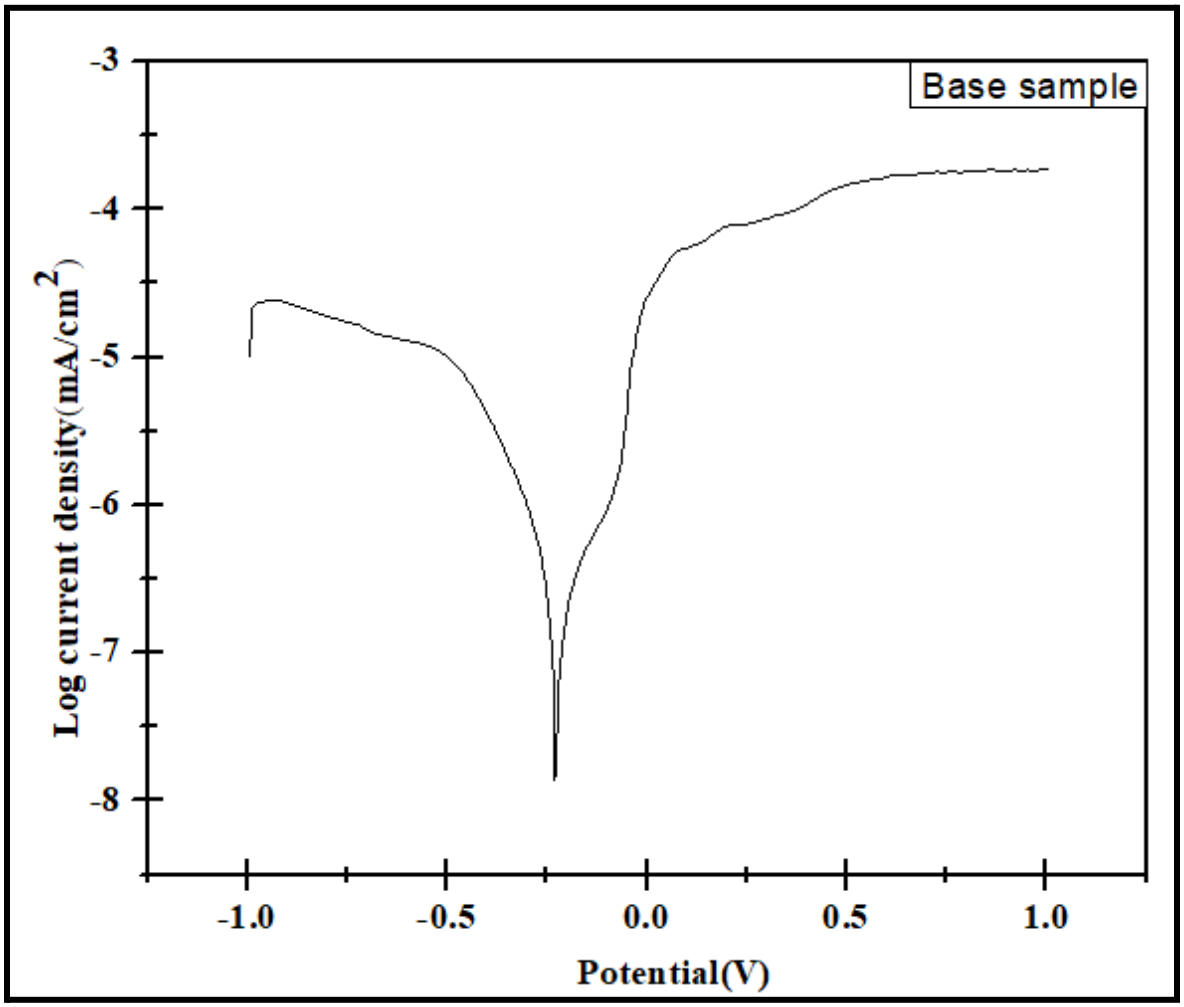


Fig. 31: Electrochemical Corrosion Measurements of the Base Sample

From Fig. 31, it can be revealed that the electrochemical corrosion started at -0.28V and stopped at -0.16418V. Also, we know the Ecorr = -0.22616 V, the Icorr = 3.9811E-07 A, and the polarization resistance = 1.1215E05 Ω.

The following equation shows how to calculate the corrosion rate of a base sample:

$CR = (K * \Delta W)/(D * A * T)$= 0.004626mm/year.

**[**C.R.: corrosion rate (mm/year), K: constant (87.6), △W: loss weight (mg) = ( initial weight – final weight), D: metal density g/cm3, A: surface area subjected to erosion cm2, T: time of exposure to corrosion in hours**]**

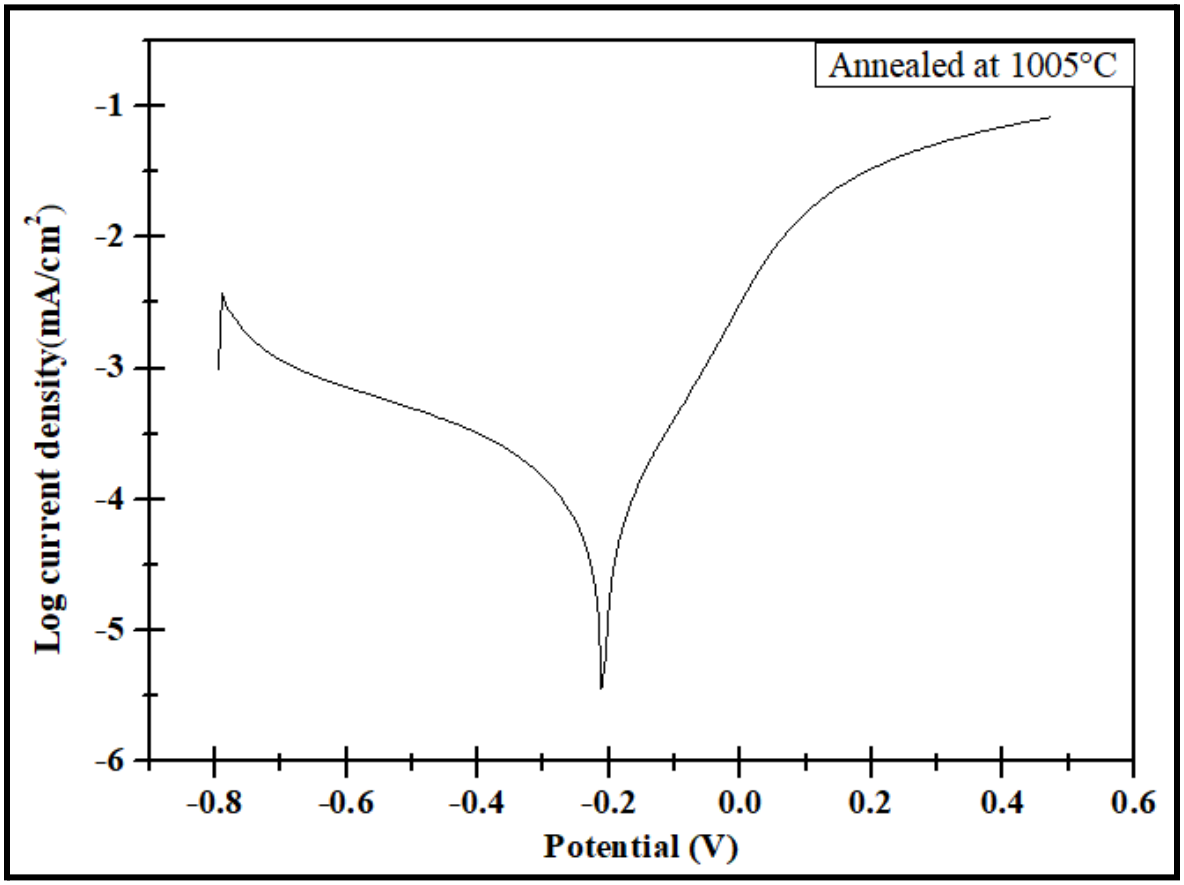


Fig. 32: Electrochemical Corrosion Measurements of the Sample Heated at 1005 °C

From Fig. 32, it can be revealed that the electrochemical corrosion started at -0.24612V and stopped at -0.17059V. Also, we know the Ecorr = -0.20806 V, the Icorr = 6.2521E-05 A and polarization resistance = 555.53 Ω

The following equation shows how to calculate the corrosion rate of the heated sample at 1005 °C:

$CR = (K * \Delta W)/(D * A * T)$= 0.72649 mm/year

The corrosion rate of the Heated sample at 1005 °C is greater than that of the base sample because the grains are coarse, so in a highly corrosive medium, this sample has a high corrosion rate.

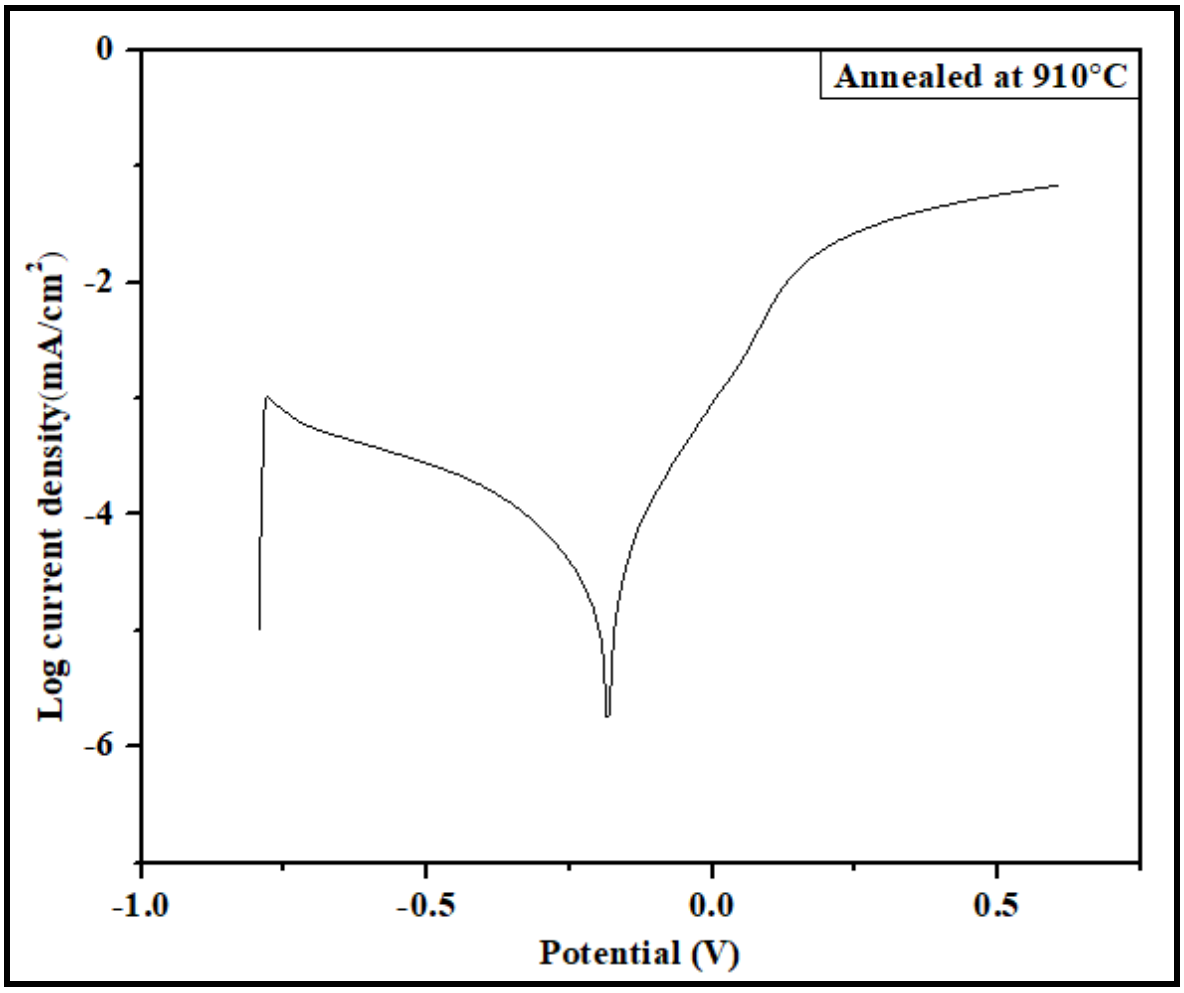


Fig. 33: Electrochemical Corrosion Measurements of the Sample Heated at 910 °C

From Fig. 33, it can be revealed that the electrochemical corrosion started at -0.24109V and stopped at -0.13535V. Also, we know the Ecorr = -0.18123 V, the Icorr = 1.8604E-05 A and polarization resistance = 1299.8 Ω

The following equation shows how to calculate the corrosion rate of the heated sample at 910 °C:

$CR = (K * \Delta W)/(D * A * T)$= 0.21618 mm/year.

The corrosion rate of the Heated sample at 910 °C is greater than the base sample because the grains are not as fine as compared to the base sample, so in a highly corrosive medium, this sample has a high corrosion rate but a lower corrosion rate than the sample heated at 1005°C.

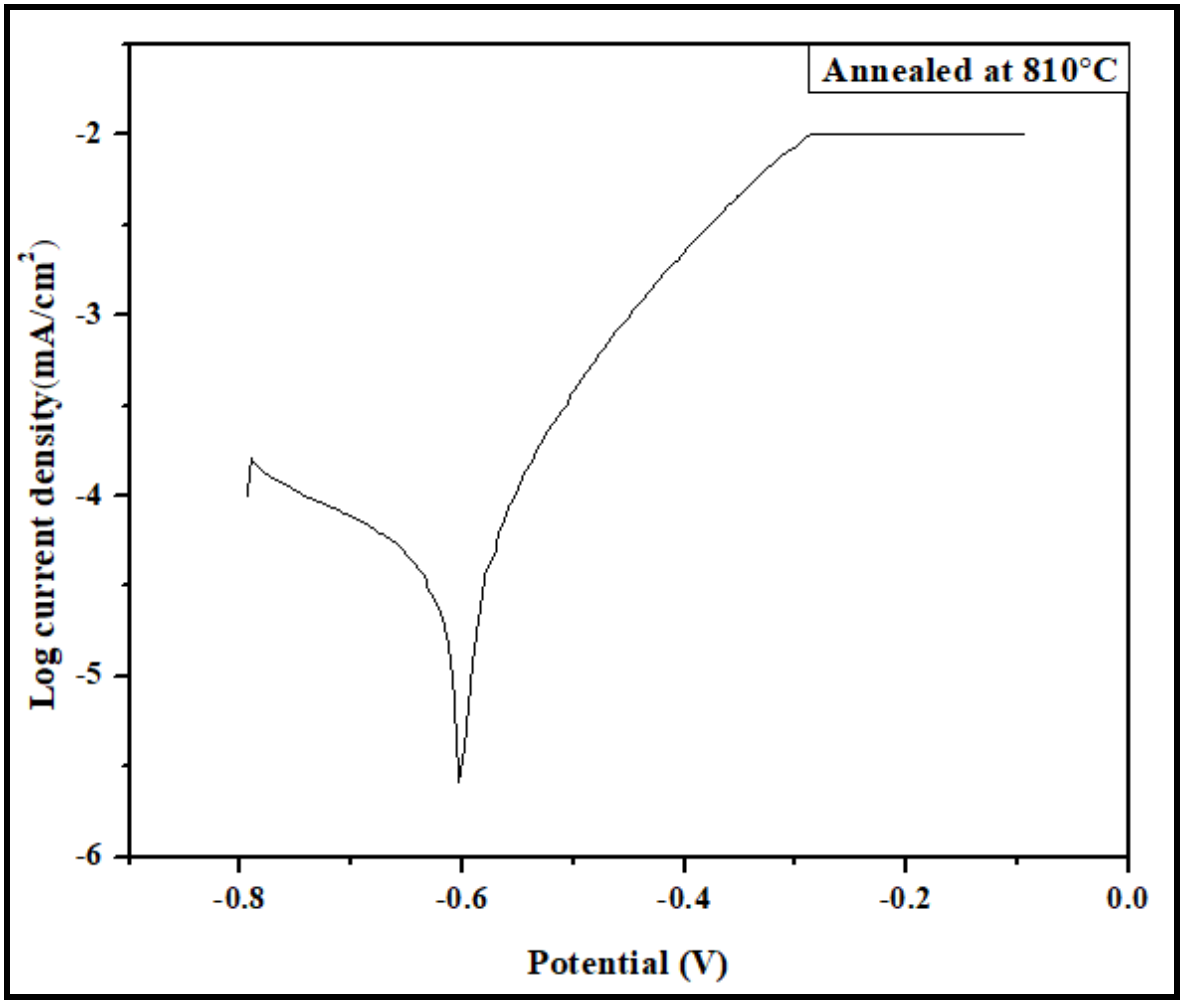


Fig. 34: Electrochemical Corrosion Measurements of the Sample Heated at 810 °C

From Fig. 34, it can be revealed that the electrochemical corrosion started at -0.61874V and stopped at -0.57846V. Also, we know the Ecorr = -0.61461 V, the Icorr = 2.9208E-05 A and polarization resistance = 738.32 Ω

The following equation shows how to calculate the corrosion rate of the heated sample at 810 °C:

$CR = (K * \Delta W)/(D * A * T)$= 0.3394 mm/year

The corrosion rate of the Heated sample at 810 °C is greater than the base sample because the grains are not as fine as the base sample, so in a highly corrosive medium, this sample has a high corrosion rate but a lower corrosion rate than the sample heated at 1005°C.

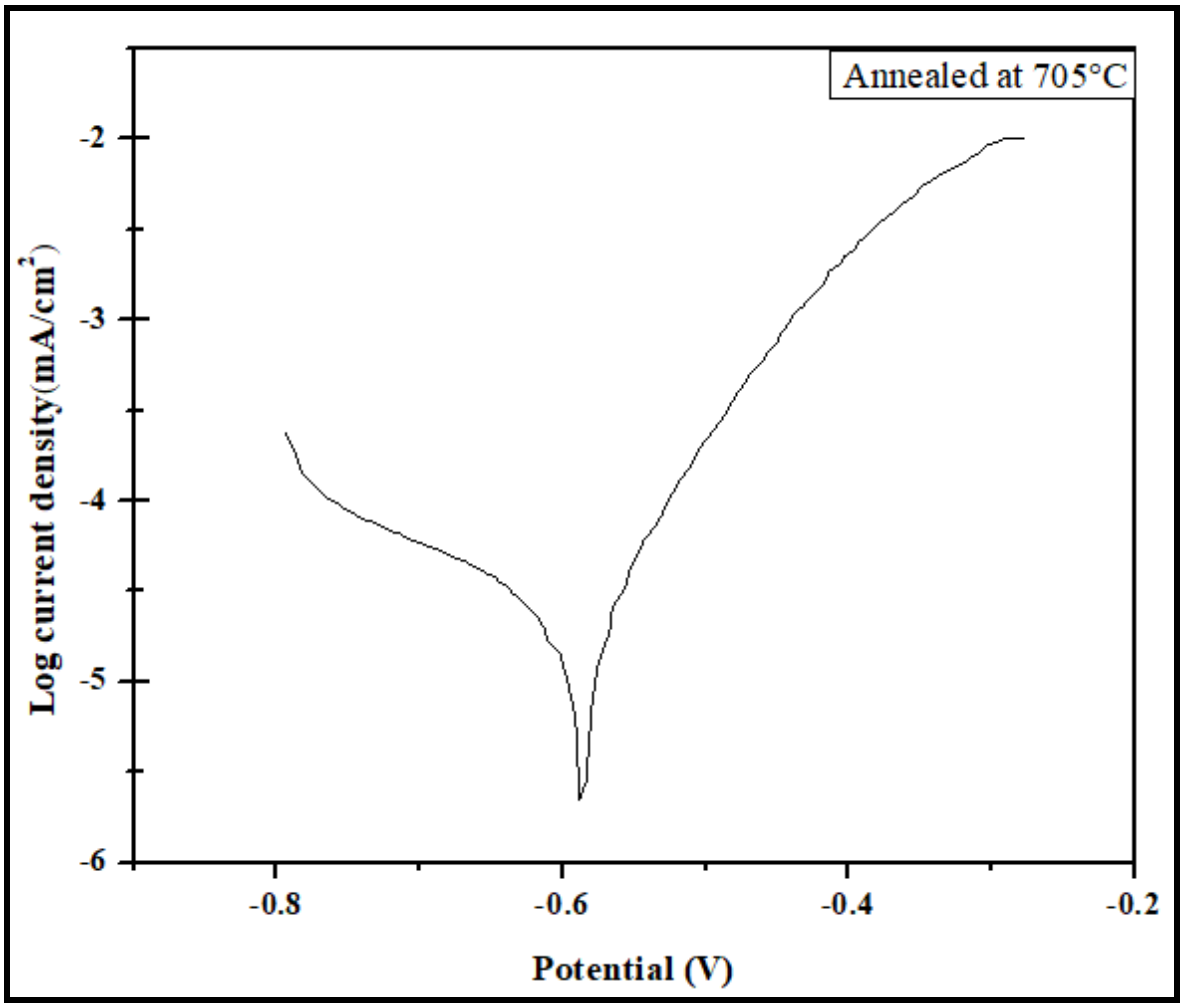


Fig. 35: Electrochemical Corrosion Measurements of the Sample Heated at 705 °C

From Fig. 35, it can be revealed that the electrochemical corrosion started at -0.5986 V and stopped at -0.56839V. Also, we know the Ecorr = -0.58853 V, the Icorr = 4.3479E-05 A and polarization resistance = 1096.7 Ω

The following equation shows how to calculate the corrosion rate of the Heated sample at 705 °C:

$CR = (K * \Delta W)/(D * A * T)$= 0.50522 mm/year

The corrosion rate of the Heated sample at 705 °C is greater than the base sample because, in the austenite phase, the grains are not as fine as compared to the base sample, so in a highly corrosive medium this sample has a high corrosion rate but a lower corrosion rate than the sample heated at 1005°C.

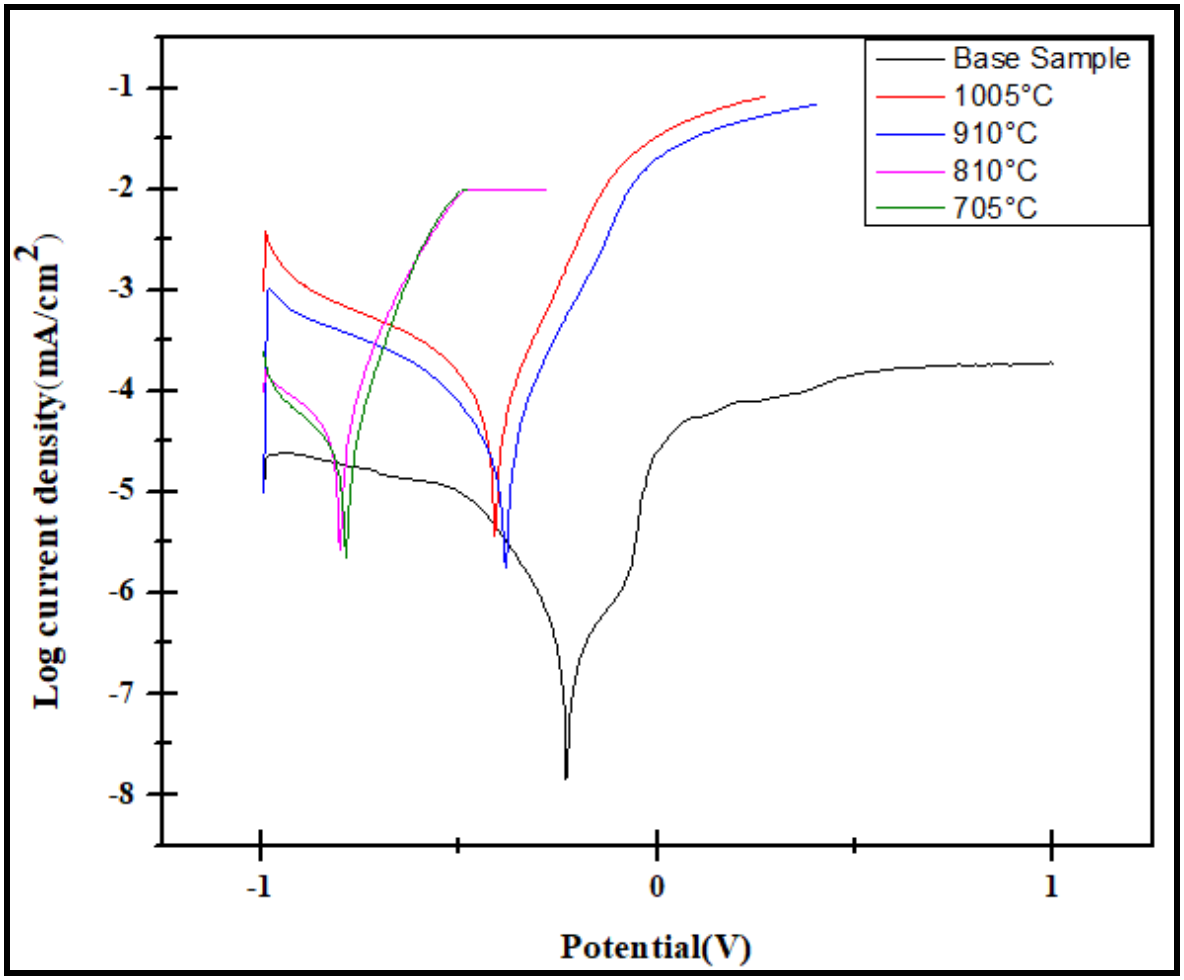


Fig. 36: Electrochemical Corrosion Measurements of All Samples

From Fig. 36, try to compare the corrosion rate and the reason behind the changes in it. Because the grains in the heated sample are coarser than those in the base sample, its corrosion rate is higher at 1005 °C, making it more corrosive than the base sample in a highly corrosive medium.

The corrosion rate of the heated sample at 910 °C is greater than the base sample because lower annealing temperatures frequently result in smaller grain sizes, which can give more grain boundaries for corrosion to occur. Smaller grains may also contain flaws that serve as locations for corrosion start, potentially resulting in a greater corrosion rate. so in a highly corrosive medium, this sample has a high corrosion rate but a lower corrosion rate than the sample heated at 1005°C.

| **Samples** | **Corrosion Rate(mm/year)** |
|---|---|
| Base sample | 0.004626mm/year |
| Heated sample at 1005 °C | 0.72649 mm/year |
| Heated sample at 910 °C | 0.21618 mm/year |
| Heated sample at 810 °C | 0.3394 mm/year |
| Heated sample at 705 °C | 0.50522 mm/year |

Table4:Corrosion Rate of Base Material and Annealed Samples

Because the grains in the heated sample at 810 °C are not as fine as in the base sample, residual stresses can cause areas of enhanced corrosion susceptibility because they cause localised deformation and strain, which promotes the corrosion rate is higher in a highly corrosive medium but lower than in the sample heated at 1005 °C.

The corrosion rate of the Heated sample at 705 °C is greater than the base sample because smaller grain sizes, which are often associated with lower annealing temperatures, can facilitate grain boundary corrosion. This is a specific type of corrosion that occurs preferentially along grain boundaries and can lead to accelerated corrosion rates, so in a highly corrosive medium, this sample has a high corrosion rate but a lower corrosion rate than the sample heated at 1005°C.

### *8.8Scanning electron microscopy analysis of corroded samples of base material and heat-treated rail steel samples:*

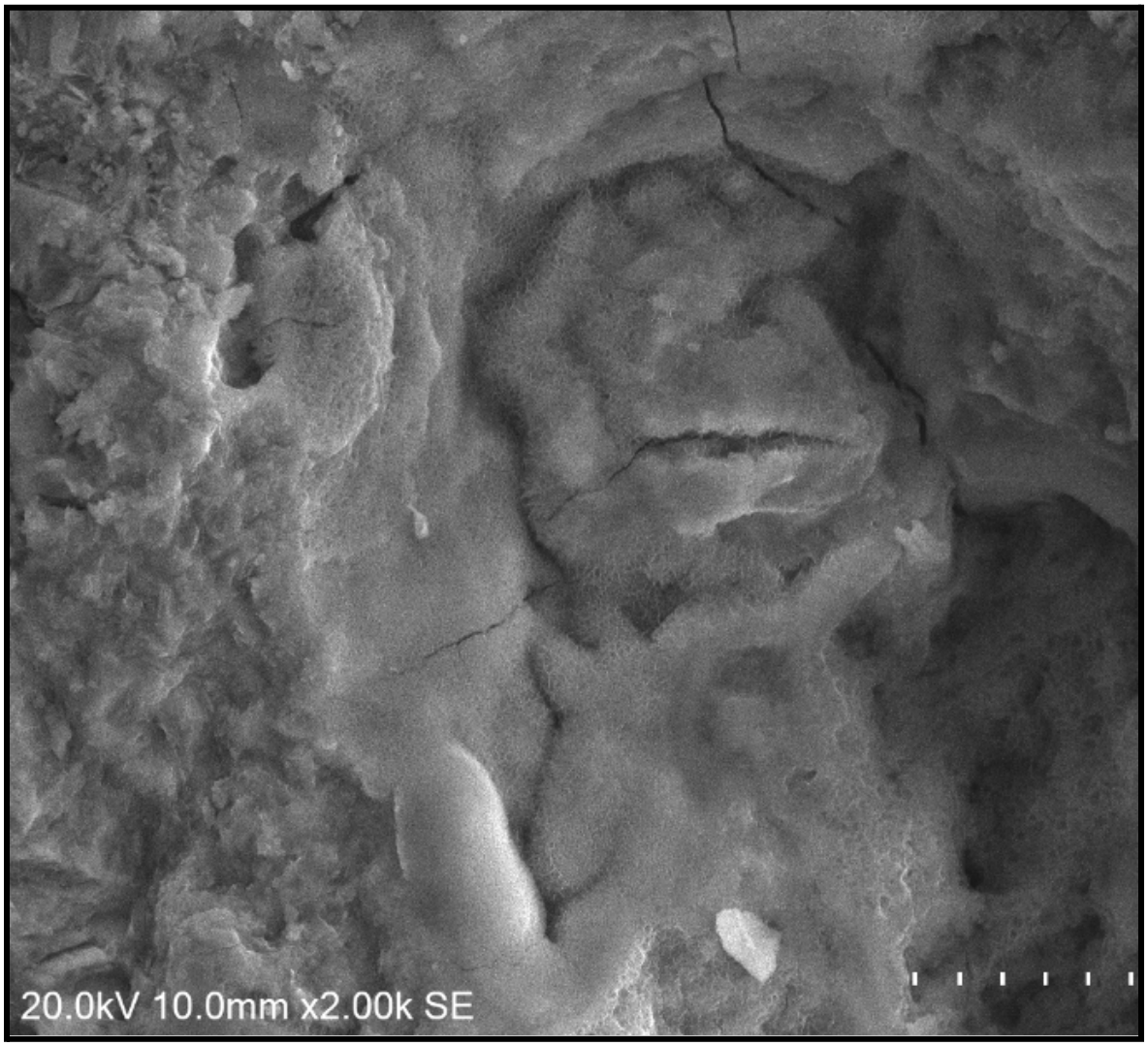


Fig. 37: SEM image of base sample after corrosion test with 2000x magnification

From Fig. 37, it can be revealed that some hairline cracks were generated by the corrosion test. This type of crack is not too harmful for railway use. Also, we found the lifeline/corrosion rate of this sample to be 0.004626mm/year.


Fig. 39: SEM image of the heat-treated sample at 910 °C after corrosion test with 2000x magnification

From Fig. 39, it can be revealed that cracks were generated by the corrosion test. This type of crack is harmful for railway use because the crack length and width are greater than the base sample but smaller than the heat-treated sample at 1005 °C. Also, we found the lifeline/corrosion rate of this sample to be 0.21618 mm/year. So this sample will corrode faster than the base sample but slower than heat treated sample at 1005 °C.

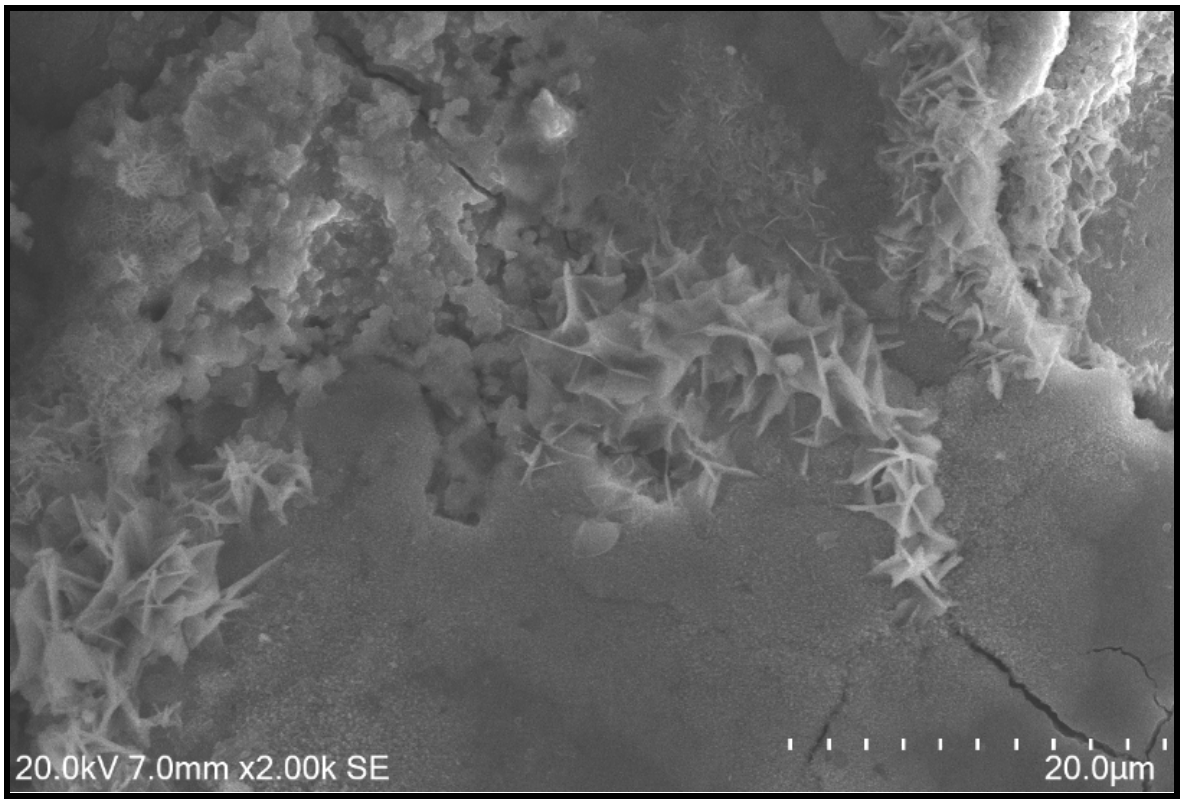


Fig. 40: SEM image of the heat-treated sample at 810 °C after the corrosion test with 2000x magnification

From Fig. 40, it can be revealed that cracks were generated by the corrosion test. This type of crack is harmful for railway use because the crack length and width are greater than the base sample but smaller than the heat-treated sample at 1005 °C. Also, we found the lifeline/corrosion rate of this sample to be 0.3394mm/year. So this sample will corrode faster than the base sample but slower than the heat-treated sample at 1005 °C and 910 °C.

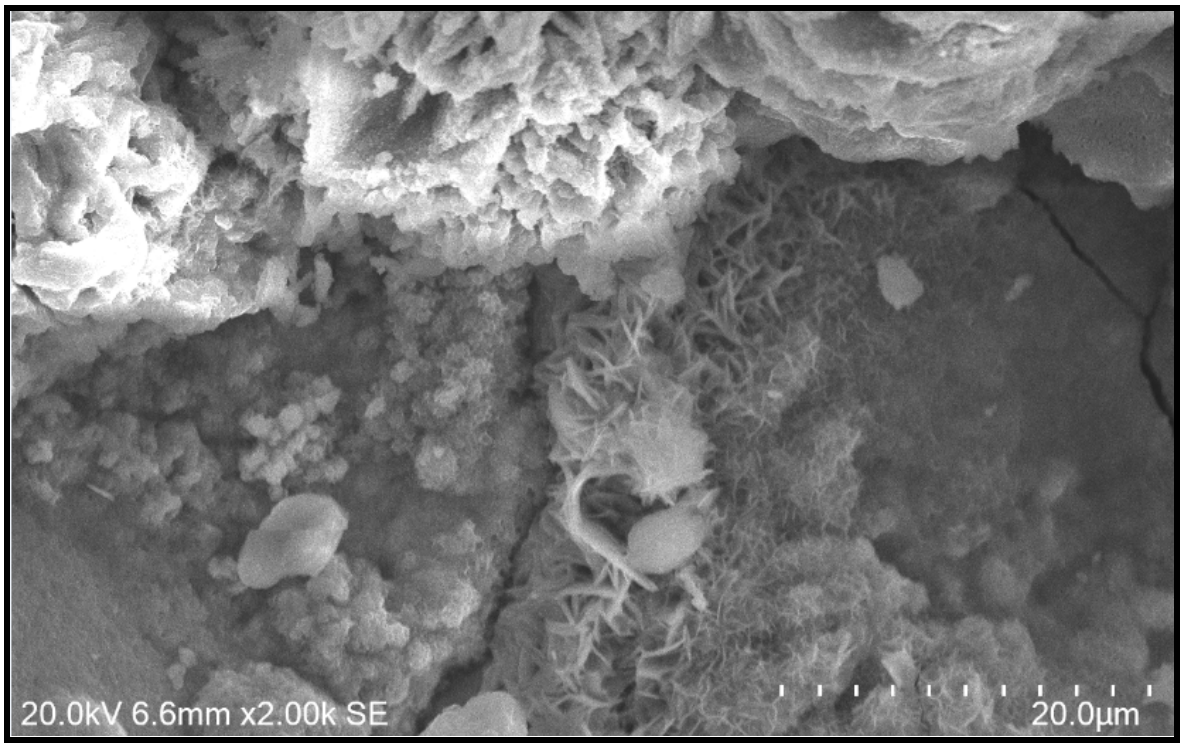


Fig. 41: SEM image of the heat-treated sample at 705 °C after the corrosion test with 2000x magnification

From Fig. 41, it can be revealed that cracks were generated by the corrosion test. This type of crack is dangerous for railway use because the crack length and width are greater than the base sample but smaller than the other heat-treated samples. Also, we found the lifeline/corrosion rate of this sample to be 0.50522mm/year. So this sample will corrode faster than the base sample and the heat-treated sample at 810 °C but slower than the other heat-treated samples.

### *8.9 Corrosion test of the base material substrate and heat-treated rail steel samples at different pH levels:*

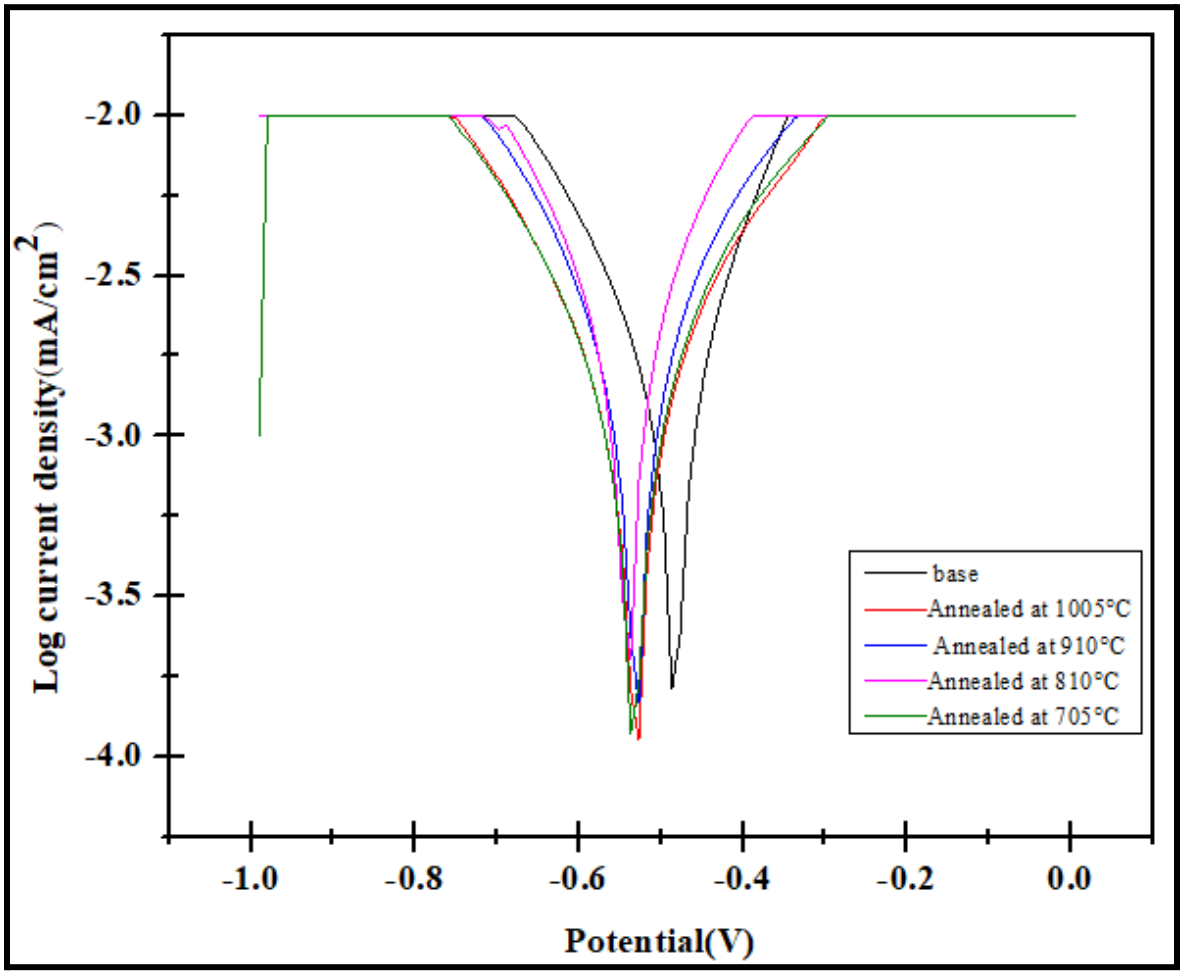


Fig. 42: Electrochemical Corrosion Measurements of All Samples at pH 1.5

From Fig. 42 and Table 5, it has been observed that decreasing annealing temperature on the corrosion rate in sulfuric acid (pH 1.5) was dependent on various factors such as microstructure, passive film formation, microchemical segregation, grain boundary corrosion, residual stresses, reaction kinetics, dissolution of alloying elements including the steel composition, the exact annealing process.

| Samples | Corrosion Rate(mm/year) |
|---|---|
| Base sample | 18.564 |
| Heated sample at 1005 °C | 39.865 |
| Heated sample at 910 °C | 61.048 |
| Heated sample at 810 °C | 34.706 |
| Heated sample at 705 °C | 67.777 |

Table 5: Corrosion Rate of Base Material and Annealed Samples at pH1.5

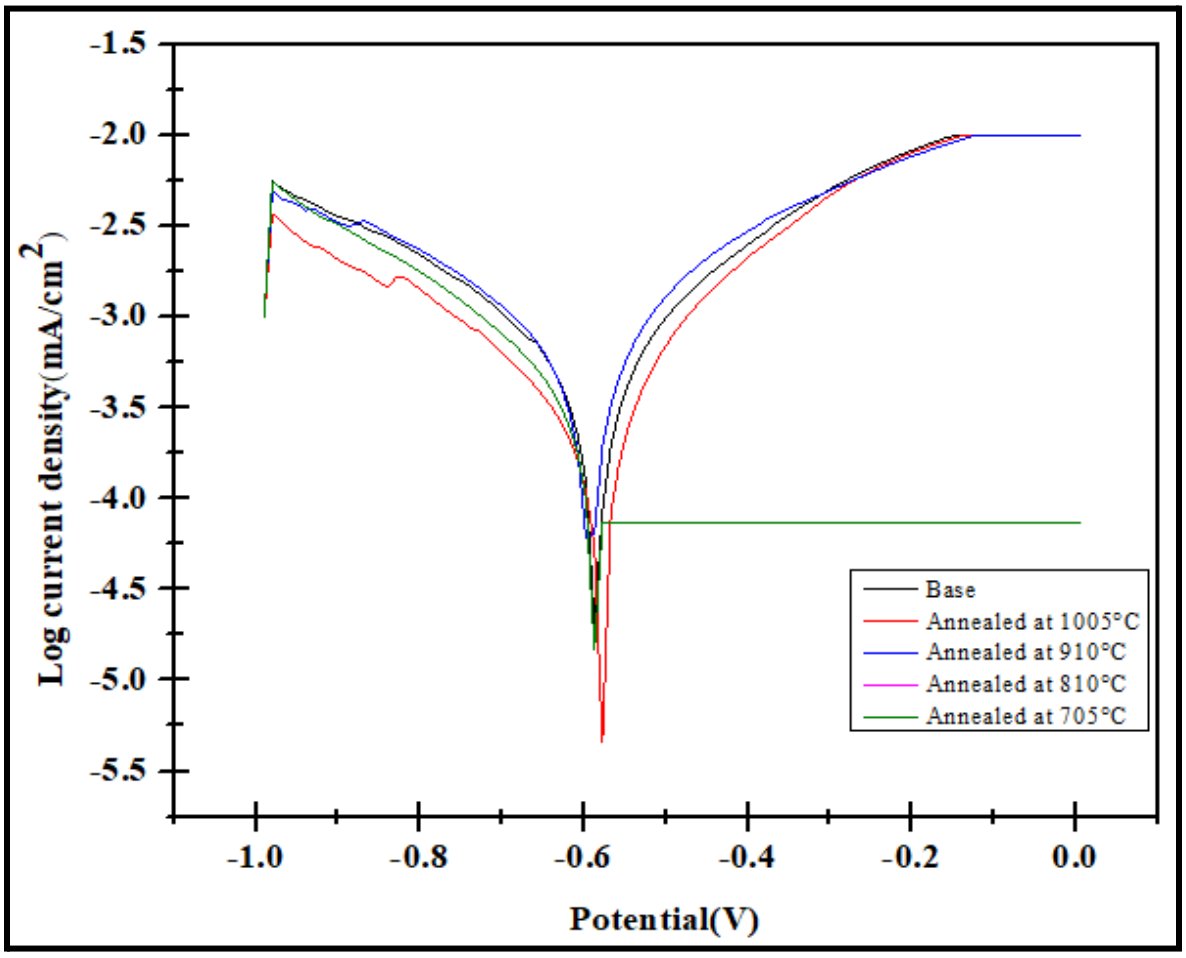


Fig. 43: Electrochemical Corrosion Measurements of All Samples at pH 2.7

According to Fig. 43 and Table 6, the corrosion rate of all samples at pH 2.7 is smaller than the corrosion rate of all samples at pH 1.5. Furthermore, the effect of decreasing annealing

temperature on the corrosion rate in sulfuric acid (pH 2.7) was dependent on a variety of factors including microstructure, passive film formation, microchemical segregation, grain boundary corrosion, residual stresses, reaction kinetics, dissolution of alloying elements including the steel composition, and the precise annealing process.

| **Samples** | **Corrosion Rate(mm/year)** |
|---|---|
| Base sample | 12.739 |
| Heated sample at 1005 °C | 7.88 |
| Heated sample at 910 °C | 33.165 |
| Heated sample at 810 °C | 17.593 |
| Heated sample at 705 °C | 10.564 |

Table 6: Corrosion Rate of Base Material and Annealed Samples at pH2.7

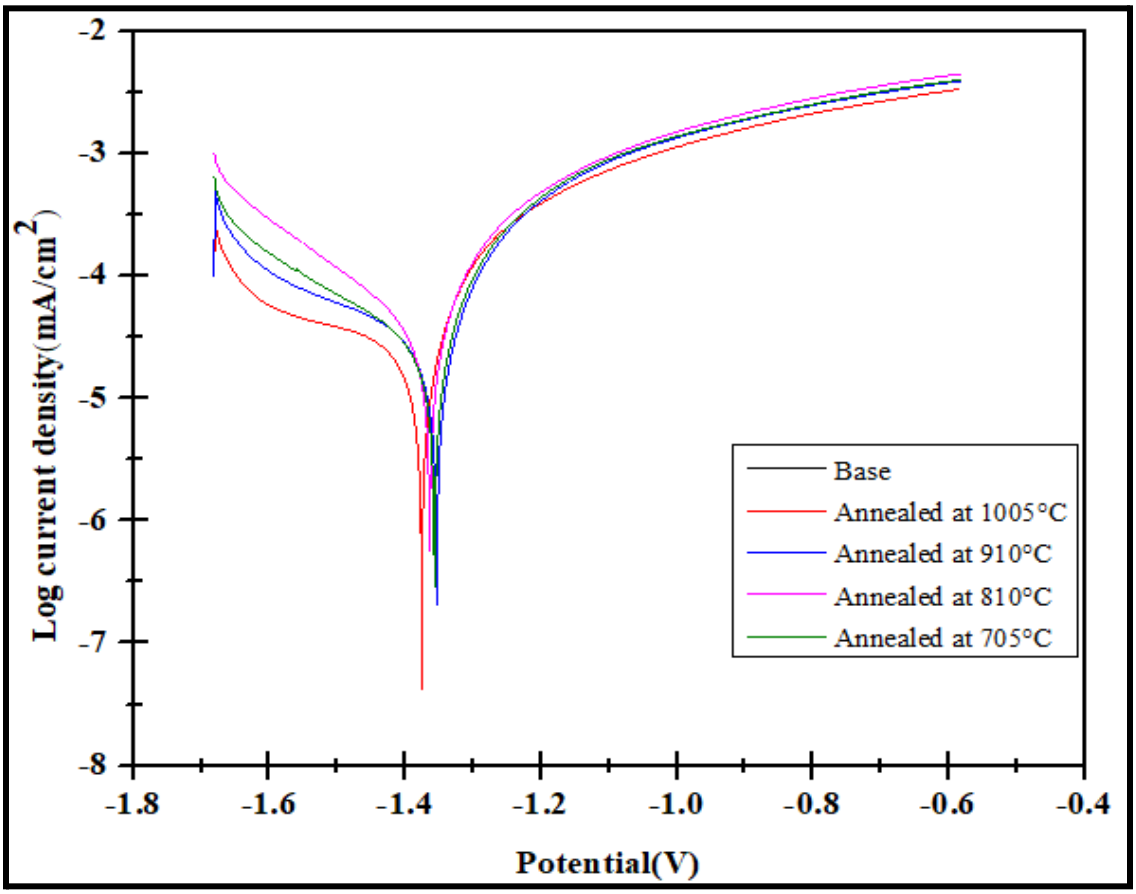


Fig. 44: Electrochemical Corrosion Measurements of All Samples at pH 3.9

According to Fig. 44 and Table 7, the corrosion rate of all samples at pH 3.9 is less than the corrosion rate of all samples at pH 2.7. Furthermore, the effect of decreasing annealing temperature on the corrosion rate in sulfuric acid (pH 3.9) was dependent on a variety of factors including microstructure, passive film formation, microchemical segregation, grain boundary corrosion, residual stresses, reaction kinetics, dissolution of alloying elements including the steel composition, and the precise annealing process.

| **Samples** | **Corrosion Rate(mm/year)** |
|---|---|
| Base sample | 1.3765 |
| Heated sample at 1005 °C | 1.4479 |
| Heated sample at 910 °C | 3.3902 |
| Heated sample at 810 °C | 1.3063 |
| Heated sample at 705 °C | 4.7642 |

Table 7: Corrosion Rate of Base Material and Annealed Samples at pH3.9

## *8.10 Optical microscopy analysis of corroded samples of base material and heat-treated rail steel samples*

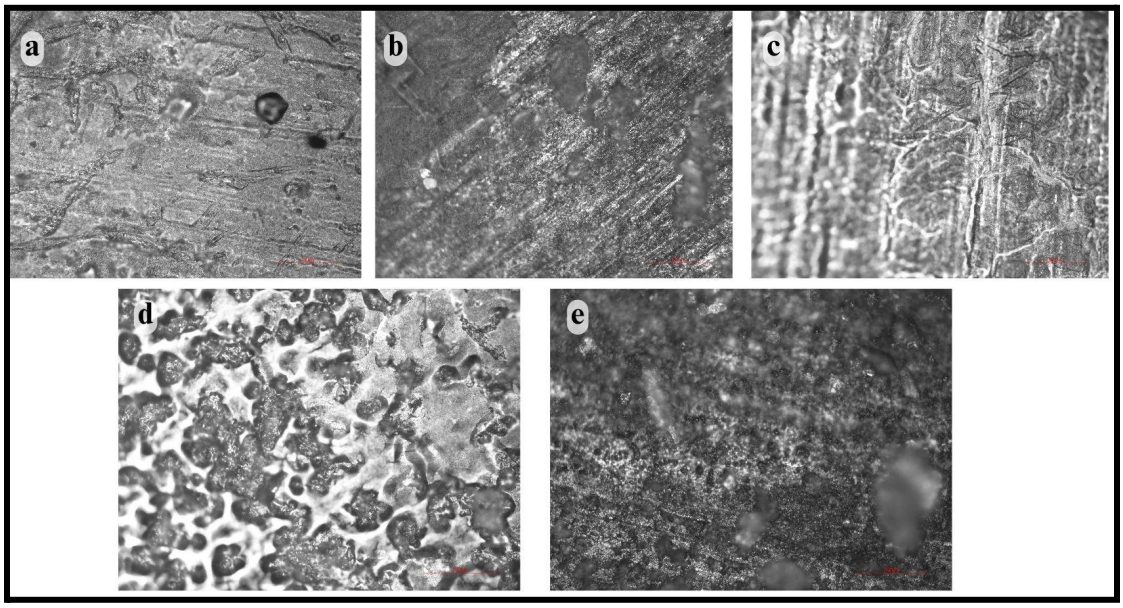


Fig 45: Optical microscopic image of all the corroded samples at pH 1.5 with 500x magnification, a-heated sample at 705 °C, b-heated sample at 810 °C, c-heated sample at 910 °C, d-heated sample at 1005 °C, e-Base sample

According to table 5 and Fig 45, it has been showing that at pH1.5 of $H_2SO_4$ solution, the highly corroded samples are heated sample at 705 °C and heated sample at 910 °C but in heated sample at 810 °C and heated sample at 1005 °C has less corrosion rate than other heated samples. Because at high acid concentrations (pH-1.49), there is a propensity for a strong passive layer to develop on the surface of the specimen, resulting in an increase in yield strength. Tensile strength decreases with increasing corrosion rate in an acidic environment. This is due to the fact that the passive layer metal bond is not robust under high-stress levels. As a result, the passive layer may have no effect on tensile strength.

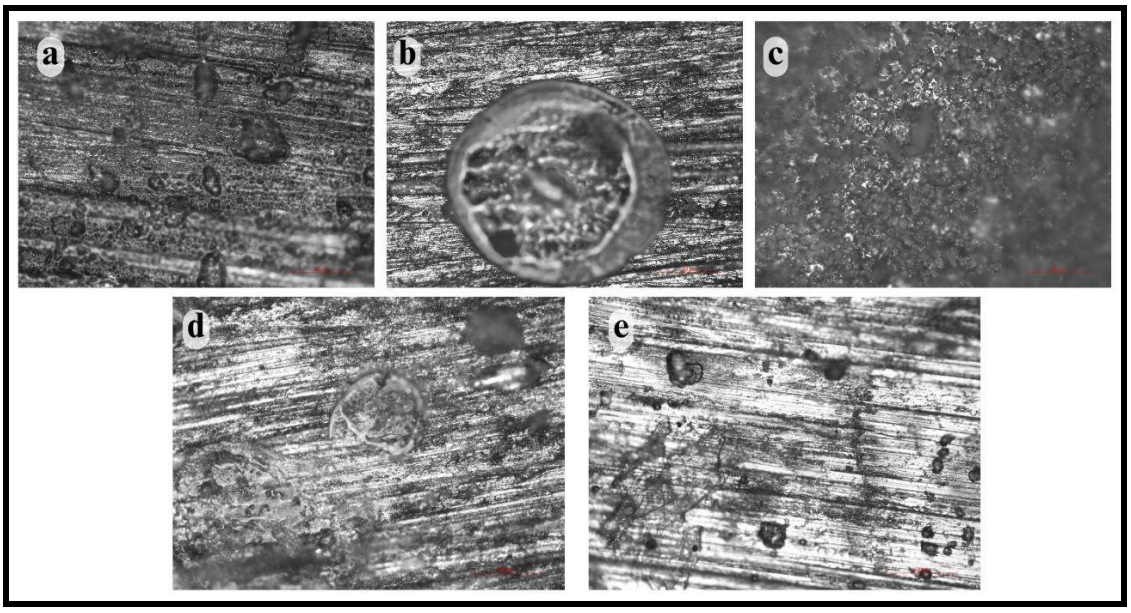


Fig 46: Optical microscopic image of all the corroded samples at pH 2.7 with 500x magnification, a-heated sample at 705 °C, b-heated sample at 810 °C, c-heated sample at 910 °C, d-heated sample at 1005 °C, e-Base sample

According to Table 6 and Fig 46, the corroded samples had a lower corrosion rate at pH2.7 of H2SO4 solution than heated corroded samples at pH1.5 of $H_2SO_4$ solution. At high acid concentrations (pH-2.7), a strong passive layer forms on the surface of the specimen, leading to an increase in yield strength. In an acidic environment, tensile strength diminishes as the corrosion rate increases. This is because the passive layer metal bond is not resistant to high stress levels. As a result, the passive layer may be ineffective in terms of tensile strength.

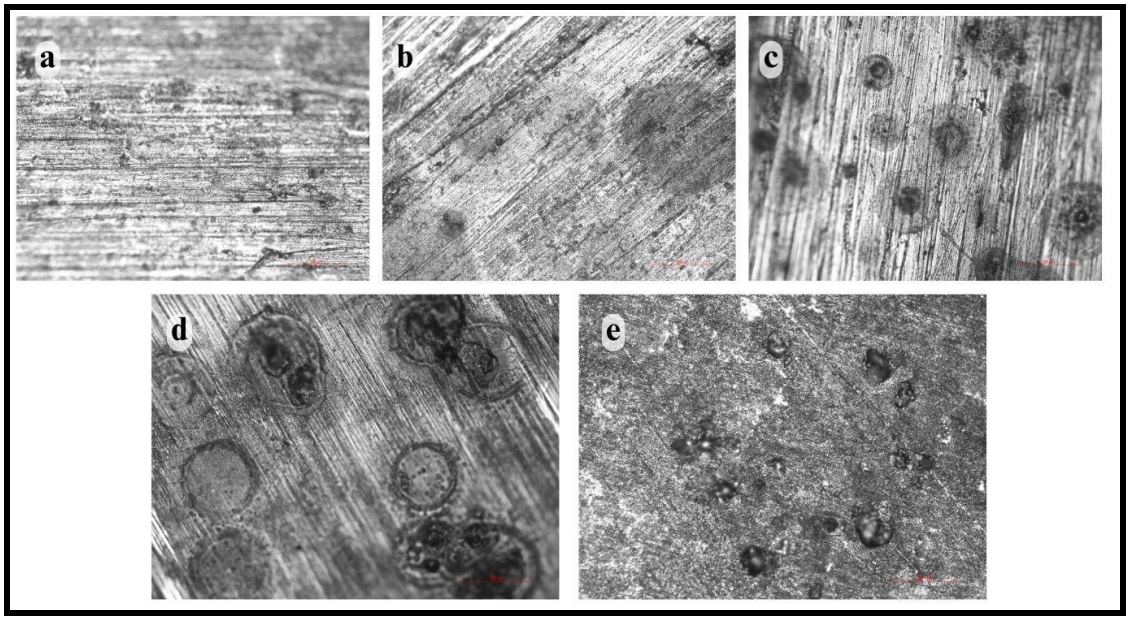


Fig 47: Optical microscopic image of all the corroded samples at pH 3.9 with 500x magnification, a-heated sample at 705 °C, b-heated sample at 810 °C, c-heated sample at 910 °C, d-heated sample at 1005 °C, e-Base sample

Table 7 and Fig 47 shows that corroded samples had a lower corrosion rate at pH3.9 of H2SO4 solution than heated corroded samples at pH2.7 of $H_2SO_4$ solution. At high acid concentrations (pH-3.9), a strong passive layer forms on the surface of the specimen, increasing yield strength. Tensile strength decreases with increasing corrosion rate in an acidic environment. This is due to the fact that the passive layer metal bond is not resistant to high-stress levels. As a result, the passive layer may be inefficient in terms of tensile strength.

## Conclusion:

This study investigated the annealing heat treatment processing to develop new microstructural features with the aim of studying the corrosion rate in 3.5wt% NaCl solution and the various pH levels of $H_2SO_4$ solution of rail steel, which is of great interest for railway service. As received rail sample, contains carbon, silicon, sulfur, phosphorus, and manganese are present at 0.67%, 0.16%, 0.01%, 0.01%, and 1.10%, respectively. After the annealing process base sample and four annealed samples were observed by optical microscope and scanning electron microscope. At the annealed temperature of 1005°C the elongated grains and fine grains have been observed. The pearlite phase is present in all samples but retained austenite was present in

the sample annealed at 810 °C and spheroidization of the pearlite phase was present in the annealed 705 °C sample. Annealed heat treatment also affected Vicker's microhardness number, with the decreasing of heat treated temperature the hardness has been decreased due to bigger grain sizes, incomplete phase transitions, uneven carbon distribution, residual stresses, and changes in the distribution of alloying elements. In the NaCl solution, the corrosion rates were different because of the specific type of corrosion that occurs preferentially along grain boundaries and can lead to accelerated corrosion rates. In another corrosive medium of the various pH levels of $H_2SO_4$ solution where corrosion rate decreased with the increasing pH level.. AS the annealed temperature increases grain refinement occurs and stress relief also occurs. From the observation of the corrosion test results, it has been confirmed that the corrosion rate of annealed rail steel decreases with increasing the annealed temperature at different Ph levels. Surface modification technologies like thermal spraying and laser cladding should be able to overcome the fault while still keeping a good corrosion-resistant layer on rail steel. The development of corrosion detection technology, particularly in-situ nondestructive and contactless technologies, is as crucial as corrosion research on rail tracks.

## Reference:

[1]Websites of railway organizations and associations like the American Railway Engineering and Maintenance-of-Way Association (AREMA) and the International Union of Railways (UIC).

[2] Effect of Heat Treatments on the Corrosion Resistance of Carbon Steel Using Salt Water , International Journal on Engineering, Science and Technology, Volume 4, Issue 1, 2022 ISSN: 2642-4088

[3] Heat Treatment and Corrosion Behavior of Selected Steels in 3.5M Sodium Chloride American Journal of Engineering Research (AJER) e-ISSN: 2320-0847 p-ISSN : 2320-0936 Volume-5, Issue-5, pp-231-237

[4] Heat Treatment Effect on Carbon Steel Corrosion Resistance at Different Carbon Content, Journal of Mechanical Engineering Research and Developments ISSN:1024-1752 CODEN: JERDFO Vol. 43, No. 5, pp. 231-237 Published Year 2020

[5] Investigating the performance of rail steels ,Daniel Herbert Woodhead, University of Huddersfield, Queensgate, Huddersfield, West Yorkshire, HD1 3DH

[6] Micromechanical characterisation of Indian rail steel ,Jay Prakash Srivastava*, Prabir Kumar Sarkar, Abhinav Gautam, Rajkumar Yadav,Hemant Kumar ,Department of Mechanical Engineering, Indian Institute of Technology (ISM) Dhanbad,Jharkhand-826004

[7] Application of isothermal heat treatment for perlite rail-steel ,Jaroslaw Konieczny 2017,Inżynieria Materiałowa 2 (216) (2017) 8287DOI 10.15199/28.2017.2.4© Copyright SIGMA-NOT

[8] Microstructural analysis and fatigue fracture behavior of rail steel ,Reza Masoudi Nejad , Khalil Farhangdoost , and Mahmoud Shariati ,Faculty of Engineering, Department of Mechanical Engineering, Ferdowsi University of Mashhad, Mashhad, Iran ,MECHANICS OF ADVANCED MATERIALS AND STRUCTURES https://doi.org/10.1080/15376494.2018.1472339

[9] Microstructure and wear resistance of pearlitic rail steels ,Author links open overlay panelAlberto J. Perez-Unzueta, John H. Beynon ,Department of Engineering, University of Leicester, University Road, Leicester LEI 7RH UK Available online 27 January 2003.

[10]High strength rail steels—The importance of material properties in contact mechanics problems ,Peter Pointner ,Voestalpine Schienen GmbH, Kerpelystraße 199, A-8700 Leoben, Austria ,Article history:Accepted 3 March 2008 Available online 5 June 2008

[11]Image analysis of pearlite spheroidization based on the morphological characterization of cementite particles, Authors:Nicolas Nutal, CRM Group, Cedric Gommes, Fonds de la Recherche Scientifique (FNRS), BLACHER SILVIA, POUTEAU PHILIPPE ,June 2010Image Analysis and Stereology 29(2),DOI:10.5566/ias.v29.p91-98,LicenseCC BY-NC 4.0

[12]Effect of Silicon on the Spheroidization of Cementite in Hypereutectoid High Carbon Chromium Bearing Steels, Kwan-Ho Kim*, Jae-Seung Lee, and Duk-Lak Lee

Technical Research Laboratories, POSCO, 1 Goedong-dong, Nam-gu, Pohang-si, Gyeongbuk 790-875, Korea. Met. Mater. Int., Vol. 16, No. 6 (2010), pp. 871~876, Doi: 10.1007/s12540-010-1203-4 Published 27 December 2010

[13]Corrosion behaviour of S500AW railway steel in a simulated industrial atmospheric environment-Hao Zhang1, Jialiang Song1, Zhaoliang Li1, Junhang Chen1, Wei Yu2, Chenghui Yin1, Chaofang Dong1and Kui Xiao1,/ Int. J. Electrochem. Sci., 17 (2022) Article Number: 220964, doi: 10.20964/2022.09.67

[14]Study on Corrosion Behavior of Pearlitic Rail Steel/S. Samala,*, A. Bhattaacharyy

and S.K. Mitra, Journal of Minerals & Materials Characterization & Engineering, Vol. 10, No.7, pp.573-581, 2011, jmmce.org

[15]Corrosion of rail tracks and their protection/ February 2021CORROSION REVIEWS 39(1):1-13/ DOI:10.1515/corrrev-2020-0069, Authors: Weichen Xu- Chinese Academy of Sciences, Binbin Zhang-Institute of Oceanology Chinese Academy of Sciences